© 2021. Published by The Company of Biologists Ltd | Journal of Cell Science (2021) 134, jcs254763. doi:10.1242/jcs.254763

REVIEW

SUBJECT COLLECTION: IMAGING

# Luminescence lifetime imaging of three-dimensional biological objects

**Ruslan I. Dmitriev[1,*], Xavier Intes[2] and Margarida M. Barroso[3,*]**

## ABSTRACT

A major focus of current biological studies is to fill the knowledge gaps between cell, tissue and organism scales. To this end, a wide array of contemporary optical analytical tools enable multiparameter quantitative imaging of live and fixed cells, three-dimensional (3D) systems, tissues, organs and organisms in the context of their complex spatiotemporal biological and molecular features. In particular, the modalities of luminescence lifetime imaging, comprising fluorescence lifetime imaging (FLI) and phosphorescence lifetime imaging microscopy (PLIM), in synergy with Förster resonance energy transfer (FRET) assays, provide a wealth of information. On the application side, the luminescence lifetime of endogenous molecules inside cells and tissues, overexpressed fluorescent protein fusion biosensor constructs or probes delivered externally provide molecular insights at multiple scales into protein–protein interaction networks, cellular metabolism, dynamics of molecular oxygen and hypoxia, physiologically important ions, and other physical and physiological parameters. Luminescence lifetime imaging offers a unique window into the physiological and structural environment of cells and tissues, enabling a new level of functional and molecular analysis in addition to providing 3D spatially resolved and longitudinal measurements that can range from microscopic to macroscopic scale. We provide an overview of luminescence lifetime imaging and summarize key biological applications from cells and tissues to organisms.

**KEY WORDS: Fluorescence lifetime, Imaging, Three dimensional**

## Introduction

In the past decade, there has been a surge of interest in imaging methodologies capable of measuring luminescence lifetime, which previously had been restricted to a small community of physicists and engineers. Luminescence lifetime is an intrinsic characteristic of any endogenous or exogenous luminescent biomolecule (luminophore), including endogenous molecules (autofluorescence), (in)organic dyes, fluorescent proteins, nanosensors and other types of biosensor probes (Fig. 1A; Box 1). Depending on its molecular structure, a luminophore can exhibit either fluorescence (with a lifetime of pico- to nano-seconds) or phosphorescence (with a lifetime of micro- to milli-seconds), and the methods to observe these two are designated as fluorescence lifetime imaging (FLI) and phosphorescence lifetime microscopy (PLIM), respectively (Fig. 1A).

[1]Tissue Engineering and Biomaterials Group, Department of Human Structure and Repair, Faculty of Medicine and Health Sciences, Ghent University, Ghent 9000, Belgium. [2]Department of Biomedical Engineering, Center for Modeling, Simulation and Imaging for Medicine (CeMSIM), Rensselaer Polytechnic Institute, Troy, NY 12180-3590, USA. [3]Department of Molecular and Cellular Physiology, Albany Medical College, Albany, NY 12208, USA.

*Authors for correspondence (Ruslan.Dmitriev@UGent.be; barrosm@amc.edu)

R.I.D., 0000-0002-0347-8718; X.I., 0000-0001-5868-4845; M.M.B., 0000-0002-0407-3181

FLI methodologies can be integrated into traditional fluorescence imaging approaches, including widefield, confocal, multiphoton, super-resolution and light-sheet microscopy, as well as macro-imaging, fluorescence molecular tomography (FMT) and other optical imaging-based approaches (Ishikawa-Ankerhold et al., 2012; Meyer-Almes, 2017; Sarder et al., 2015; Denicke et al., 2007; Becker et al., 2017; Hirvonen and Suhling, 2020; Le Marois and Suhling, 2017; Datta et al., 2020; Poudel et al., 2020; Wang et al., 1992). FLI can also be combined with more specialized approaches such as Förster resonance energy transfer (FRET), which enables sensing of nanoscale interactions. (Fig. 1; Box 1) (Abe et al., 2013; McGhee et al., 2011; Piston and Kremers, 2007; Rajoria et al., 2014; Bunt and Wouters, 2017). In contrast to measurements of fluorescence intensity, lifetime measurements are independent of the fluorophore concentration (above the required threshold) and are minimally affected by the tissue optical properties. Thus, lifetime imaging provides an absolute value that is directly related to the luminophore structure and to how this structure is affected by environmental changes, such as temperature, pH, polarity and mechanical forces (Fig. 1B). Modern FLI and PLIM platforms cover an optical resolution ranging from sub-micrometer to several millimeters, a spectral range from 180 to 1700 nm and a time-domain resolution from sub-picoseconds to milliseconds, with measurement speeds that range from real-time for one-photon FLI and PLIM (Raspe et al., 2016; Trinh et al., 2019; Cheng et al., 2020) to several minutes per frame for two-photon PLIM (Rytelewski et al., 2019). By allowing quantitative, multiparameter and often non-invasive and non-destructive three-dimensional (3D) analyses of live cells and tissues to be performed, FLI and PLIM provide a broad support to the ongoing '3D molecular-imaging revolution'.

A number of comprehensive reviews have described the technology underlying FLI and PLIM (Ishikawa-Ankerhold et al., 2012; Hirvonen and Suhling, 2020; Le Marois and Suhling, 2017; Levitt et al., 2009; Becker et al., 2017; Berezin and Achilefu, 2010; Dmitriev, 2017; Periasamy, 2001; Trinh et al., 2019), but they rarely address the benefits and applications of these powerful imaging approaches to researchers with training in biology and biomedical sciences. This Review aims to fill this gap by introducing readers to the FLI, PLIM and FLI–FRET-based methodologies that are important for multiparameter 3D imaging of cells, tissues and small animals, with a brief demonstration of the underlying biosensing technologies. Moreover, we will highlight the growing need for '3D FLI', specifically in cancer and stem cell biology, developmental processes, intravital imaging, super-resolution microscopy, host–pathogen interactions and other areas of cell and molecular biology.

## Luminescence lifetime imaging – a window into the molecular environment of 3D cells and tissues

Life inside the human body is seldom less than 3D. Subcellular organelles, cells, biofilms and tissues, all classically pictured as flat

Journal of Cell Science (2021) 134, jcs254763. doi:10.1242/jcs.254763

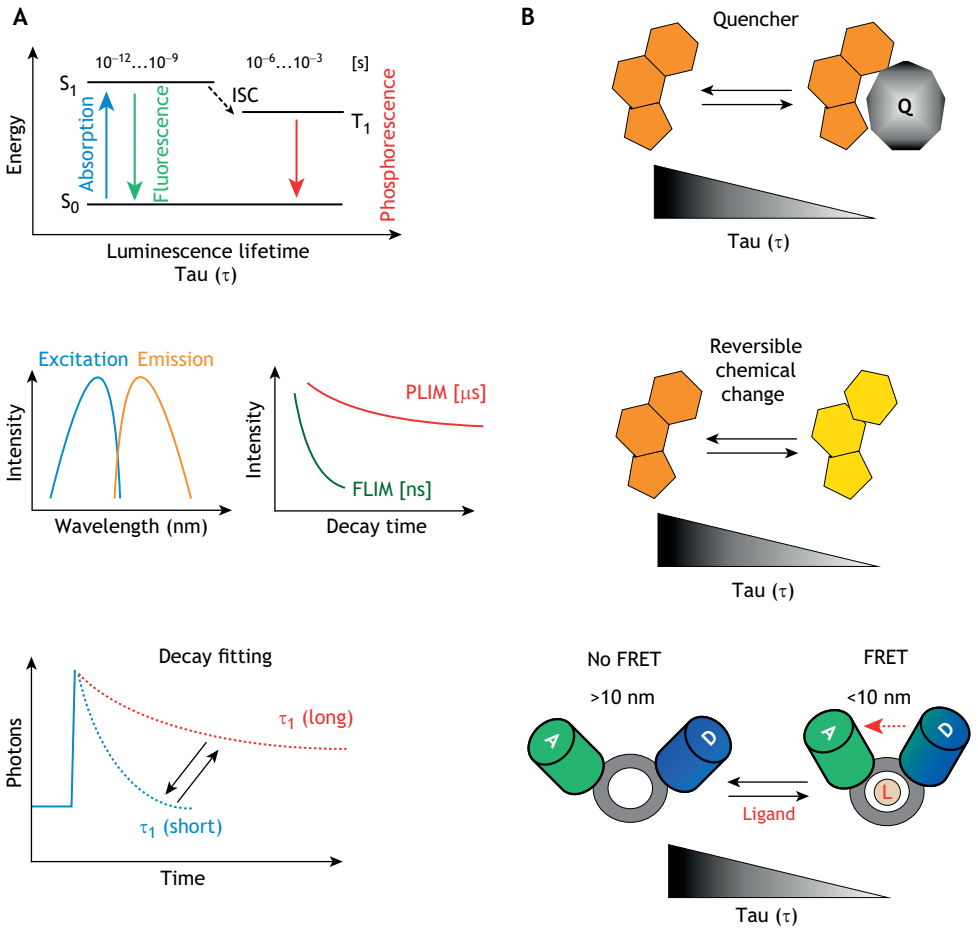


**Fig. 1. Brief introduction into FLIM, FRET and PLIM.** (A) Interaction of luminescent molecules with light results in fluorescence or phosphorescence (top panel), measured either in spectral intensity (left middle panel) or decay times (also known as 'lifetimes', Tau; right middle panel). In turn, luminescence lifetime can be measured using FLIM (nanoseconds) or PLIM (microseconds) (right middle panel). Importantly, the same molecule can change its lifetime, as shown by decay fitting, due to quenching and other interactions, which can be used in biosensing (bottom panel). In the top panel, S0 indicates singlet ground state, S1 indicates singlet excited state and T1 indicates triplet excited state. ISC, intersystem crossing. (B) Examples of sensing methodologies employed in FLIM and PLIM with illustration of the effects of the presence of quencher (top; e.g. molecular oxygen in PLIM), reversible changes in molecular structure of the fluorophore (middle; e.g. pH sensing by FLIM) and ligand binding by the FLIM–FRET biosensor (bottom). A, acceptor; D, donor; L, ligand; Q, quencher.

entities in textbooks and other scientific literature, overwhelmingly display, when imaged *in vivo*, significantly different 3D features, including shapes, dimensions and surface-to-volume ratios. Importantly, the 3D spatial (*x*,*y*,*z*) and temporal (*t*) organization and morphology of the nucleus, mitochondria, cytoskeleton, and the endo-lysosomal and biosynthetic membrane trafficking pathways, as well as microenvironmental parameters (viscosity, pH and others), are key features for the establishment of higher-complexity cellular processes, including cell migration, signaling, metabolism and proliferation in non-disease and pathological tissues (Wu et al., 2018; Pampaloni et al., 2007; Liu et al., 2018a; Ovečka et al., 2018; von Erlach et al., 2018; Rios and Clevers, 2018; Libanje et al., 2019; Wang et al., 2020). 3D organization influences the spatial distribution of surface receptors and confers biophysical and/or mechanical features that affect responses to different stimuli. The physics of cell–cell and cell–matrix interactions are highly dependent on the three-dimensionality of cells and tissues (Page et al., 2013; Teodori et al., 2017; Laurent et al., 2017). Three-dimensionality is also critical for native tissue organization, the function of a stem cell niche, developmental processes, and for applications in regenerative medicine (tissue engineering) and tumor biology, as well as for drug delivery, pharmacological research and other areas of biomedical science. Thus, the need to visualize cells and tissues in 3D has driven research and innovation to further develop quantitative advanced imaging technologies. In particular, luminescence lifetime (FLI and PLIM) imaging provides a unique molecular window into cells and tissues, bringing us closer to achieving the overall goal of comprehensive quantitative 3D imaging of live biological samples at the nanometer scale (Fig. 1; Box 1). Advances in manufacturing exogenous phosphorescent and fluorescent dyes, proteins, bioconjugates and biosensors, as well as improved characterization of endogenous fluorescence features, have allowed for the luminescence-based sensing of a plethora of physiological processes, structural components and biomarkers, ranging from protein–protein interactions to tissue oxygenation (Table 1) (Berezin and Achilefu, 2010; Blacker and Duchen, 2016; Quaranta et al., 2012; Sarder et al., 2015; Steinegger et al., 2020; Datta et al., 2020; Papkovsky and Dmitriev, 2013, 2018b; Conway et al., 2017; Rajoria et al., 2014).

Generally, '3D imaging' of biological materials (e.g. *ex vivo* or *in vivo* systems, tissue engineered scaffolds, organoids and small model organisms) is performed by stacking data acquired in a two-dimensional (2D) mode (*x*,*y*) using optical sectioning or widefield detection. In this type of applications, the contrast acquired is confined to the plane imaged, and the sample is scanned sequentially plane by plane to obtain the third dimension. 3D stacking and reconstruction can then be achieved computationally for subsequent 3D analysis (Datta et al., 2020; Le Marois and Suhling, 2017) (Fig. 2). These approaches are mainly associated with microscopy techniques that are used on transparent and/or thin samples, allowing for good light penetration depth (Cheng et al., 2020). However, when considering intact biological tissues, scattering becomes a prevalent phenomenon, precluding the ability to confine the detected photon to a localized 2D plane. Hence, the 3D nature of light propagation needs to be considered. 3D imaging can be achieved via solving a mathematical inverse

Journal of Cell Science (2021) 134, jcs254763. doi:10.1242/jcs.254763

**Box 1. FLI terms and detection modalities**

Luminescence is a physical phenomenon that encompasses both fluorescence and phosphorescence imaging approaches (Fig. 1A). There are a wide variety of microscopy and macroscopy imaging setups that enable the measurement of luminescence lifetimes of luminophores (i.e. a fluorophore or phosphor) in the visible and NIR wavelength range, with impact in many biomedical fields. Fluorescence lifetime imaging (FLI) includes microscopy-based approaches, described as FLIM (fluorescence lifetime imaging microscopy), and macroscopy-based optical imaging, described as MFLI (macroscopy fluorescence lifetime imaging). Phosphorescence lifetime imaging microscopy is referred to as PLIM.

While fluorescence intensity displays relative magnitude effects that are typically associated with the local concentration of the molecule, luminescence lifetime provides a 'fingerprint' of the fluorophore and/or phosphorescent dye structure in relationship to the external environment (sensing). The aim of luminescence lifetime measurements is to quantify the lifetime, $\tau$ (tau), which provides information about the immediate physical, chemical and biological environment of the luminophore, effectively making any luminophore a sensing probe. Thus, the measurement of lifetime changes using FLI or PLIM can detect the occurrence of molecular events, such as conformational changes of proteins induced by changes in the physical, chemical and biological environment surrounding the luminophore, which can be included in fluorescent proteins or conjugated to a wide variety of proteins (see figure). In the case of FLI, the lifetime values are within ~0.1–20 ns, whereas phosphorescence lifetimes (measured using PLIM) are typically sensed in the 'slower' range of 1–1000 µs.

FLI and PLIM can be combined with FRET, a nanometer-range proximity assay that informs on protein–protein interactions occurring within 1–10 nm range, or used for other applications. Importantly, FLI and PLIM provide molecular information independently of the spatial resolution delivered by the imaging setup used to collect the data (see figure for a comparison of spatial resolution and depth of penetration for a variety of imaging modalities. CM, confocal microscopy; IVM, intravital microscopy; LISH, light sheet imaging; MFMT, mesoscopic FMT; MPM, multiphoton microscopy; SRM, super-resolution microscopy). For example, incorporating FLI–FRET assays into low-resolution optical imaging techniques, such as FMT, allows for the investigation of nanometer-range molecular interaction in intact animals, as shown for NIR MFLI deep-tissue imaging (Fig. 3).

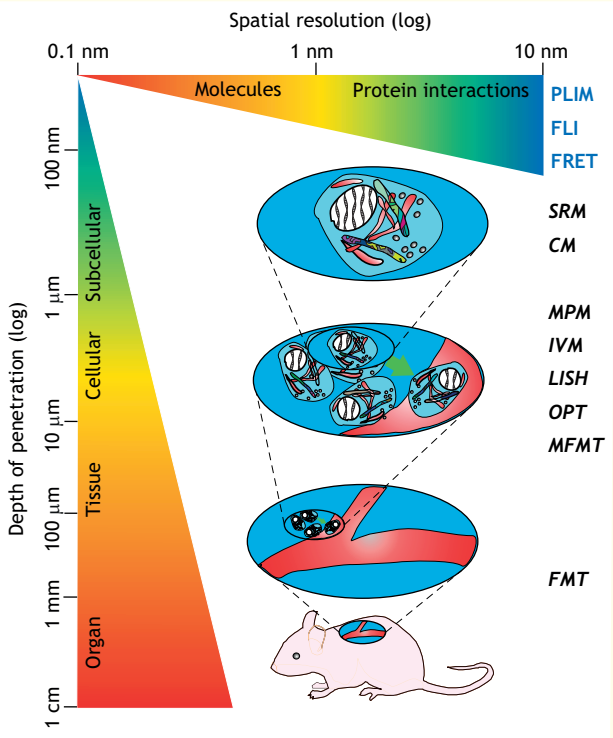


problem that is centered around a 3D light propagation model to directly generate 3D volumes, such as in optical projection tomography (OPT) or FMT (Ozturk et al., 2016; Venugopal et al., 2012; Ntziachristos, 2010; Yoon et al., 2020) (Fig. 3). Although these approaches require an increased level of processing and expertise, and lead to reduced resolution images, they offer the unique potential to image large volumes in deep tissues, enabling the monitoring of biological processes over organs and/or whole organisms.

## Biological and biomedical applications of FLI, FRET and PLIM

### Imaging metabolism and cell death in cancer and stem cells

Optical metabolic imaging was introduced over four decades ago in the form of autofluorescence imaging of the cell redox status, firstly using fluorescence intensity measurements (Barlow and Chance, 1976) and more recently leveraging lifetime contrast imaging (Lakowicz et al., 1992). The field has seen a significant revival owing to the wide availability of multiphoton fluorescence lifetime microscopy (FLIM) (Masters et al., 1998; Ranawat et al., 2019; König, 2020). On the application side, the balance between cell energy production pathways (i.e. oxidative phosphorylation and glycolysis) has been shown to reflect cancer and stem cell function (Blacker and Duchen, 2016; Brand and Nicholls, 2011; Vander Heiden et al., 2009; Rodríguez-Colman et al., 2017). The vast majority of optical metabolic imaging studies employ two-photon FLIM of endogenous NAD(P)H, sometimes combined with the detection of FAD and other co-factors (Blacker and Duchen, 2016; Ghukasyan and Kao, 2009; Liu et al., 2018b; Ranawat et al., 2019; Skala et al., 2007; Stringari et al., 2012; Digman et al., 2008; Alam et al., 2017). NAD(P)H in its free form displays a short fluorescence lifetime, indicative of glycolysis, whereas longer emission lifetimes that result from the binding of NAD(P)H to enzymes are indicative of an involvement in oxidative phosphorylation or other metabolic processes (Blacker et al., 2014). Depending on the subcellular localization, cell type, interactions with cellular enzymes and proteins, or presence of metabolites in medium, the observed lifetimes of NAD(P)H can be discriminated and even calibrated, thus allowing the distinction between NADH and NADPH (Blacker et al., 2014; Leben et al., 2019). The main disadvantages of autofluorescence imaging are the inability to always measure the absolute amounts of redox co-factors (especially in objects with multiple cell types) and a lack of correlation with other markers of cell metabolism, such as glycolytic and oxygen consumption rates (assessed by measuring oxygenation using the PLIM method) and membrane polarization (assayed by staining with membrane potential-sensitive dyes) (Table 1) (Brand and Nicholls, 2011; Foster et al., 2006; Okkelman et al., 2020b; Perottoni et al., 2020 preprint). Nevertheless, autofluorescence FLIM can discriminate between different metabolic states and has been recently applied to T cell classification using the 'random forest' machine learning approach (Walsh et al., 2020). Because it is based on two-photon excitation, the method is intrinsically useful for *in vitro* analysis of 3D multicellular systems, such as spheroids, tumoroids and organoids, as well as *in vivo* imaging of transparent specimens or exposed tissues (Wetzker and Reinhardt, 2019; Datta et al., 2020; Gómez et al., 2018). Recently, following the pioneering work of Szulczewski et al. (2016), metabolic autofluorescence FLIM measurements have been used to discriminate the spatial and temporal heterogeneity related to macrophage polarization in co-culture with primary human invasive ductal carcinoma cells (Heaster et al., 2020). So far, most of these studies have focused

**Table 1. Biological processes and biomolecules measured using FLI(M) and PLIM**

| Biological parameters | Sensing principle | Examples of biosensor probes used, and microscopes required |
|---|---|---|
| Molecular oxygen ($O_2$) and hypoxia | Quenching of phosphorescence (PLIM), fluorescence or delayed fluorescence of various types of exogenous, endogenous and/or FRET-based biosensors. Enables absolute quantitative measurements over a broad range of biological models, from cultured cells to *in vivo*. | (1) General overview of optical $O_2$ sensing methodologies (Dmitriev and Papkovsky, 2012, 2015; Papkovsky and Dmitriev, 2018a, 2013, 2018b; Quaranta et al., 2012; Roussakis et al., 2015; Wang and Wolfbeis, 2014; Yoshihara et al., 2017).<br>(2) Vascular two-photon excited PLIM-compatible cell-impermeable dendrimeric probe Oxyphor-2P (Esipova et al., 2019). Requires custom-made two-photon PLIM.<br>(3) Cell permeable conjugated polymer nanosensors, working in ratio- and PLIM-detection modes (Dmitriev et al., 2015a). Broadly compatible with conventional confocal microscopes and with two-photon and PLIM systems.<br>(4) Small molecule Pt–Glc phosphorescent conjugate with optimized performance for imaging spheroids and intestinal organoids (Dmitriev et al., 2014; Okkelman et al., 2020c). Requires commercially available confocal PLIM. |
| Redox status, sometimes referred to as optical metabolic imaging | FLIM analysis of the autofluorescence derived from endogenously produced NAD(P)H and FAD, dependent on their interaction with cellular proteins. Alternatively, this can be performed using genetically-encoded redox biosensors. | (1) No exogenous probe required, but this method can greatly benefit from co-staining with dyes or the presence of fluorescent proteins (Datta et al., 2020). A two-photon FLIM microscope is required.<br>(2) Fluorescent protein-based redox biosensors are also proposed, such as roGFP, NADH:$NAD^+$ ratio and others (Yellen and Mongeon, 2015; Mongeon et al., 2016). Compatible with one- and two-photon FLIM microscopes. |
| Protein interactions | Receptor–ligand binding, molecular forces, redox and other types of FRET–FLIM-based biosensors. Frequently report FRET ratios rather than absolute values. | (1) General reviews on intramolecular FLIM–FRET protein biosensors (Conway et al., 2017; Nobis et al., 2013; Timpson et al., 2011a).<br>(2) Eevee-Akt-mT2 FRET–FLIM biosensor for AKT kinase activity Conway et al. (2018). Compatible with one- and two-photon FLIM microscopes. |
| pH, $Ca^{2+}$ and other ions | Dye, nanosensor and fluorescent protein-based biosensors. Enables absolute quantitative measurements. | (1) Reviewed in Looger and Griesbeck (2012); Tian et al. (2012); Steinegger et al. (2020).<br>(2) pH-sensing enhanced cyan fluorescent protein (ECFP) (O'Donnell et al., 2018; Poëa-Guyon et al., 2013). Can be expressed endogenously or used in biosensor scaffold materials. Requires commercially available confocal FLIM.<br>(3) $Ca^{2+}$-sensing dye Oregon Green BAPTA-1 (Kuchibhotla et al., 2009; Lattarulo et al., 2011). Requires commercially available confocal or two-photon FLIM. |
| Lipids and cell membrane organization | Dye, chemical conjugate or FLIM–FRET protein-based biosensors, reporting on polarity, viscosity or protein interactions of membrane-bound biosensors. Sometimes enables absolute quantification (e.g. viscosity), but the analysis of observed quenching and luminescence lifetimes is complex. | (1) General reviews on lipid FLIM probes (Amaro et al., 2014; Owen et al., 2007).<br>(2) Nile Red dye, used for imaging polarity and lipid droplets (Levitt et al., 2015; Okkelman et al., 2020a). Suitable for spectral ratio and FLIM measurements, requires confocal or commercially available FLIM microscopes.<br>(3) BODIPY-C12 dye for FLIM sensing of viscosity (Steinmark et al., 2019). Requires commercially available confocal FLIM microscopes. |

on the 2D analysis of 3D objects, which may result in inaccuracies owing to the rather arbitrary choice of a single ($x$,$y$) 'equatorial' plane in asymmetric tumor organoids or the analysis of averaged $z$ projections.

Novel fluorescent and phosphorescent biosensor probes have been used in 'multiparametric' applications of autofluorescence-based redox imaging assays (Kalinina et al., 2016; Okkelman et al., 2020b). Thus, mitochondrial function and cell bioenergetics can be analyzed with complementary FLIM and PLIM approaches using genetically encoded NADH/$NAD^+$ redox biosensors (Hung et al., 2011), glucose biosensors (Díaz-García et al., 2019), oxygen-sensing phosphors (Dmitriev et al., 2014, 2013; Okkelman et al., 2017a,b), pH-sensing proteins and mitochondrial membrane potential-sensitive probes (Okkelman et al., 2019). FLIM in 3D has been used to measure cellular NAD(P)H within live intestinal organoids expressing the stem cell marker Lgr5–GFP, demonstrating functional differences in redox status between oxidative phosphorylation and glycolysis in stem cells and non-stem cell types, and emphasizing the need to combine FLIM measurements of NAD(P)H with $O_2$-sensing PLIM for the analysis of cell metabolism (Okkelman et al., 2020b).

Additional biomarkers and physical parameters that are important for cancer and stem cell biology (Nia et al., 2020), such as temperature (e.g. tumor-induced thermogenesis), cellular viscosity, polarity and tension, can be sensed using FLIM and

Journal of Cell Science (2021) 134, jcs254763. doi:10.1242/jcs.254763

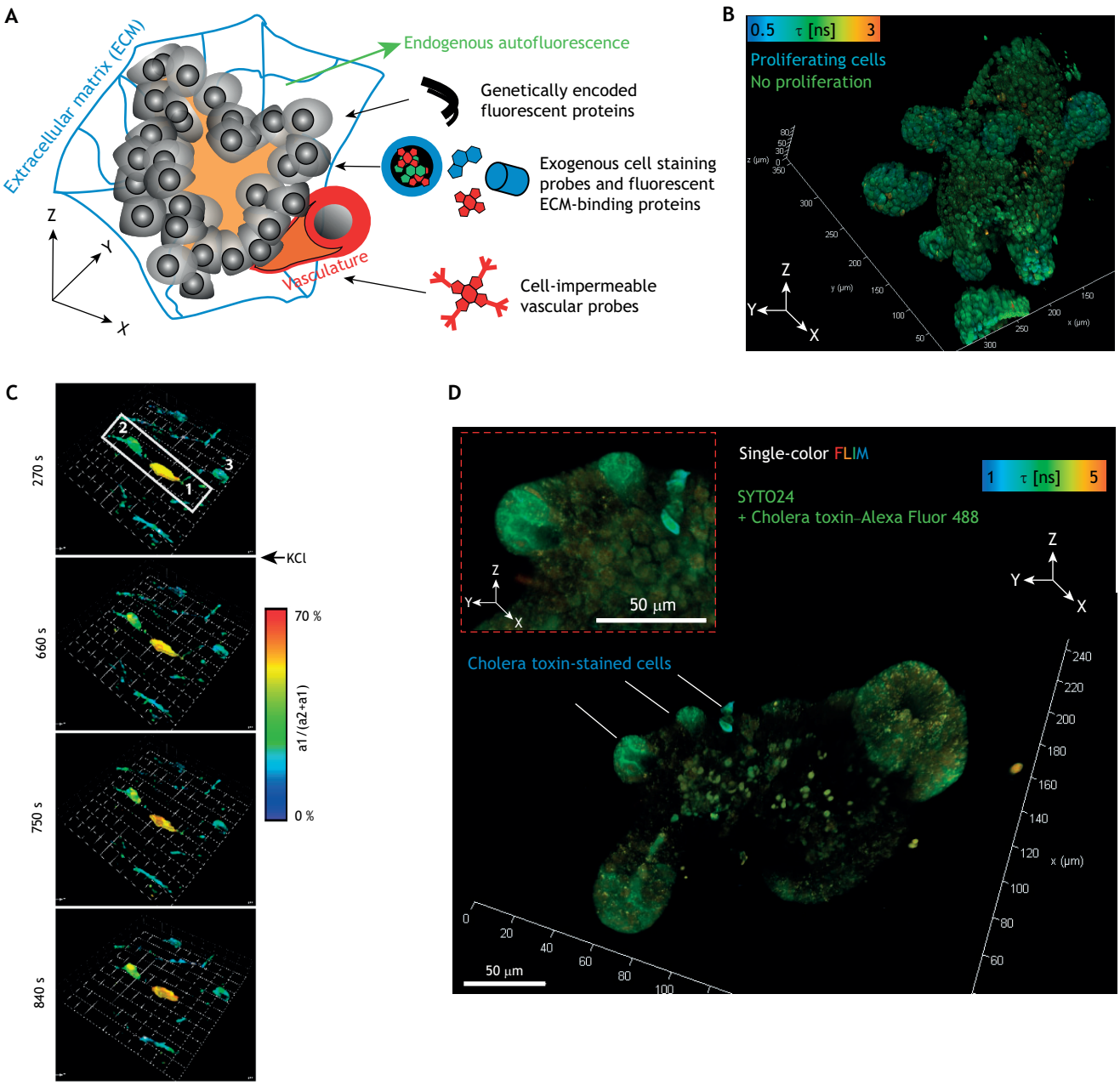


**Fig . 2. FLIM and PLIM in 3D imaging of live organoids and tissues.** (A) Schematic representation of a 3D tissue imaged using FLIM or PLIM and available biosensor probe types. (B) Two-photon excited 3D FLIM enables the visualization of proliferating (blue, crypts) and non-proliferating (green, differentiated villi regions) cells in live mouse intestinal organoids, using staining with Hoechst 33342 and BrdU pulsing. (C) Dynamic intravital 4D FRET–FLIM in the brain stem of CerT L15 mice, perfused with 100 mM KCl at the indicated time, shows the depolarization of neurons followed by a $Ca^{2+}$ increase. Colormap (0–70%) demonstrates FRET efficiency, which is proportional to the $Ca^{2+}$ increase. Numbers 1–3 indicate separate neurons with different kinetics of response. Box highlights neurons undergoing changes. Thus, the dynamics of $Ca^{2+}$ changes in live brain is measured both at the level of frequency and quantitatively. Images reproduced from Rinnenthal et al. (2013), where they were published under a CC-BY license. (D) Use of FLIM in a lifetime-domain multiplexing experiment ('Tau contrast imaging'). FLIM (single excitation with 488 nm laser) improves the contrast of live intestinal organoids that are co-stained with two dyes emitting in the same spectral window: SYTO 24 (longer lifetimes, more orange color) and cholera toxin-labeled Alexa Fluor 488 (shorter lifetimes, blue-green colors). This helps to visualize functionally different cell types. Inset shows magnified region of the organoid. The images shown in B and D were prepared in the Dmitriev laboratory, as described in Okkelman et al. (2020c).

various FRET biosensors. Temperature control is essential for cell viability, and growing evidence highlights the importance of the temperature gradients that are experienced by metabolically active biological tissues (Chrétien et al., 2018; Ogle et al., 2020; Zhou et al., 2020). Importantly, in breast and colon cancer cells, temperature gradients have been linked to the function of the uncoupling protein UCP1, mitochondrial function and cell oxygenation (Jenkins et al., 2016; Kawashima et al., 2020). Molecular tension FLIM has been used to map the cellular adhesive landscape, with biosensor probes revealing the tension forces experienced by cells (Glazier et al., 2019; Dumas et al., 2019; Ringer et al., 2017).

Cell death and proliferation are important hallmarks of cancer and developmental programs, and their detection is thus highly relevant.

Journal of Cell Science (2021) 134, jcs254763. doi:10.1242/jcs.254763

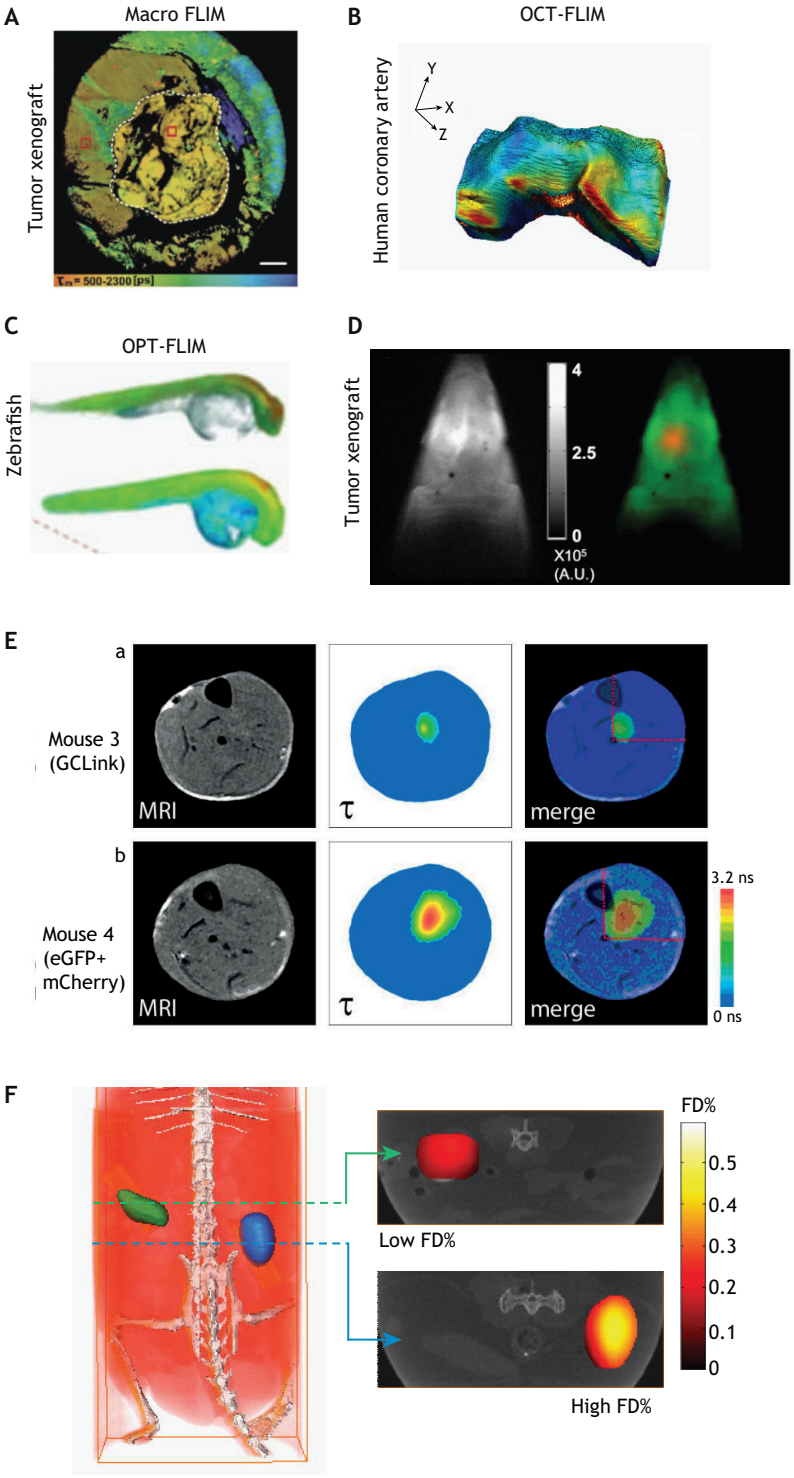


**Fig. 3. 3D FLI and FRET using macroscopy-based approaches.** (A) Fluorescence time-resolved macro-imaging of NAD(P)H autofluorescence in a tumor xenograft to assess metabolic heterogeneity at macroscale. The white dashed line marks the tumor border, and the two red boxes indicate two regions with different $\tau_m$ values, inside and outside the tumor; $\tau_m$ indicates amplitude weighted fluorescence lifetime. Scale bar: 2 mm. Image adapted with permission from Shcheslavskiy et al. (2018), ©The Optical Society. (B) OCT volume imaging superimposed with a FLIM map of the human coronary artery. *Post mortem* human coronary artery was subjected to immunofluorescence using anti-LOX-1 receptors tagged with Alexa Fluor 532-labeled secondary antibodies. LOX-1 receptors are found predominantly in the endothelial cells of the intima and are involved, upon binding to oxidized low-density lipoproteins, in the formation of lipid-rich foam cells on the artery. Image adapted with permission from Shrestha et al. (2016), ©The Optical Society. (C) OPT-rendered 3D images of zebrafish overexpressing a caspase-3 FRET biosensor and controlled by the ubiquitin promoter [Tg(Ubi:Caspase3bios)], following 25 Gy gamma irradiation to induce localized apoptosis. Top: whole OPT–FLIM data set, showing intensity merged false-color lifetime. Bottom: whole OPT–FLIM data set, showing false-color lifetime, without intensity merging, to highlight the short lifetime contribution of the yolk. Image reproduced from Andrews et al. (2016), where it was published under a CC-BY license. (D) Tomography of cancer cells expressing a NIR-fluorescent protein (iRFP720) injected into the brain to allow deep-tissue imaging. Left: planar transmission fluorescence showing autofluorescence and iRFP720 intensity levels (A.U., arbitrary units). Right: fluorescence decay amplitude images to discriminate iRFP720 lifetime (red) from tissue autofluorescence lifetime (green). Whole-body imaging of deep-seated organs is achieved by combining iRFP720 cell labeling with fluorescence lifetime contrast. Image reprinted from Rice et al. (2015) with permission from AACR. (E) Cross-sections from tomographic reconstructions of magnetic resonance imaging (MRI) and eGFP donor fluorescence lifetime from imaging of the hind legs in two live transfected mice. Panel (a) corresponds to a leg containing muscles expressing the FRET construct, GCLink, whilst panel (b) displays the non-FRETing control co-expressing eGFP and mCherry separately. Left, MRI; middle, reconstructed lifetime distribution ($\tau$); right, merged images. Dashed lines show that both mice are imaged from same perspective in MRI and fluorescence lifetime imaging. Image adapted with permission from McGinty et al. (2011), ©The Optical Society. (F) Tomographic estimate of fluorescence lifetime NIR inter-molecular FRET levels in a mouse model. Shown here are a 3D rendering of the CT images (left) and quantitative comparison of FRETing donor fraction (right) from capillary tubes implanted in the abdomen with low (green) FRET and high (blue) FRET signals (FD%, FRET donor fraction indicating FRET donors involved in FRET events.). An antibody–antigen pair, Alexa Fluor 700-labeled mouse IgG1 and Alexa Fluor 750-labeled goat anti-mouse IgG, was used to measure specific intermolecular interactions as detected by NIR FRET MFLI tomography. Images in F were generated as described in Venugopal et al. (2012), with permission from the authors.

Notably, live-cell FLIM has been used to monitor cell proliferation via quenching of 5-bromo-2′-deoxyuridine (BrdU; Fig. 2B) and the co-expression of tagged cyclin kinase inhibitor nuclear proteins (Okkelman et al., 2016; Schreiber et al., 2012). DNA damage can be measured by FLIM-based visualization of the double-strand breaks (Lou et al., 2019), and activation of apoptosis in tumor spheroids has been assessed using FRET-based expressed caspase activity biosensors or by combining $O_2$-sensing PLIM with fluorescent necrosis and dyes that report caspase-3 and/or caspase-7 activation (Dmitriev et al., 2015b). Interestingly, NADH FLIM has been used to discriminate between apoptosis and necrosis events (Wang et al., 2008).

### Protein-based FLIM–FRET biosensors for intravital imaging of the therapeutic response

The area of intravital imaging using FLIM–FRET has been pioneered in the past two decades, spurred by advances in intramolecular fluorescent protein-based FRET biosensors, which are designed to change their 3D conformation in response to the targeted biological process (e.g. phosphorylation or interaction with

other biomolecules) (Fig. 1B; Box 1). Altering the distance between the donor and acceptor fluorescent proteins in these biosensors can result in reversible changes to their donor fluorescence lifetime, hence directly reporting on the affected biological process (Table 1). FLIM–FRET has been increasingly employed *in vivo* using intravital imaging, owing to progress in the development of transgenic animals and imaging instrumentation (Nobis et al., 2013; Timpson et al., 2011a; Ellenbroek and van Rheenen, 2014). For example, Timpson and co-workers used *in vivo* FLIM–FRET to study cancer cell invasion in tumor xenografts expressing a RhoA GTPase biosensor, via implanted optical imaging windows (Timpson et al., 2011b). Currently available intramolecular FLIM–FRET biosensors enable the transient detection of different substrates (e.g. peptides, phosphorylated proteins, $Ca^{2+}$-binding proteins and posttranslational modifications) by exploiting binding domains, cleavage sites, binding tags or other ligands (Conway et al., 2018, 2017; McGhee et al., 2011). For instance, FLIM–FRET biosensors have been used in 3D cancer models to analyze activation of apoptosis (Weber et al., 2015) and to visualize AMP-activated protein kinase (AMPK) gradients in response to drug stimulation (Chennell et al., 2016). FLIM–FRET redox biosensors represent a powerful alternative to autofluorescence-based metabolic imaging (Yellen and Mongeon, 2015). FLIM–FRET has enabled the spatial monitoring of the developing kidney using deep-tissue multiplexed 3D imaging of $Ca^{2+}$ and cAMP in zebrafish embryos (Zhao et al., 2015). To advance the study of amyloid protein function in Alzheimer's disease, protein-based biosensors have been applied to monitor the development of aggresomes using FLIM and 3D structural illumination microscopy (Lu et al., 2019). As an alternative to biosensors, FLIM has been used to monitor both the kinetics of doxorubicin uptake via its quenching effect on histone H2B–eGFP (Bakker et al., 2012) and the release of doxorubicin from iron oxide nanoparticles in tumor spheroids (Basuki et al., 2013). A current limitation of FLIM is that, with some exceptions (pH-, $O_2$-, temperature- and $Ca^{2+}$-imaging), most of the research described above is based on semi-quantitative relative measurements of fluorescence lifetime. This is due to cell- and environment-specific effects on luminescence lifetime, which often preclude a precise calibration system that can be transferable to different subcellular compartments and cell types.

#### Intravital imaging of oxygenation, metabolism and $Ca^{2+}$ concentration

Measuring $O_2$ can be performed using two different imaging approaches: (1) 'bottom-up' one-photon imaging using dye- and nanosensor-based probes designed to image intracellular gradients; and (2) 'top-to-bottom' two-photon imaging using cell-impermeable dendrimer-protected porphyrin conjugates to image oxygenation in the bloodstream (Table 1). Intravital PLIM can be performed with both these two types of probes (Papkovsky and Dmitriev, 2018a,b), in addition to imaging of tissue-engineered constructs and studies of cellular $O_2$ gradients (Dmitriev et al., 2012; Finikova et al., 2008; Mik et al., 2006; Yoshihara et al., 2017; Zhou et al., 2016; Napp et al., 2011; Mizukami et al., 2020). Two-photon imaging of vascular oxygenation (Sakadžić et al., 2010) has enabled 3D intravital PLIM combined with NADH and blood flow measurements (Devor et al., 2012; Gómez et al., 2018; Esipova et al., 2019; Finikova et al., 2008; Sakadžić et al., 2010). Successful design of vascular dendrimeric probes has also helped to map bone marrow oxygenation and to study $O_2$-dependence of hematopoietic stem cell (HSC) migration (Christodoulou et al., 2020). The use of $O_2$-sensing nanoparticles *in vivo* is still rare due to their suboptimal tissue distribution and quick clearance from the bloodstream (Dmitriev et al., 2015a). Nevertheless, a recent study successfully performed intravital time-lapse multiplexed FLIM–FRET using the AKT kinase activity of the 'Eevee-Akt-mT2' biosensor and $O_2$-sensing PLIM to monitor hypoxic regions that are resistant to therapeutical targeting of the phosphoinositide 3-kinase (PI3K) pathway in pancreatic cancer (Conway et al., 2018). Similarly, modified two-photon excited PLIM (FaST-PLIM) has been used for intravital imaging of lymphocyte mobility in solid and hematological tumors in mice (Rytelewski et al., 2019).

Additional parameters that provide information on the function of excitable cells can also be sensed using FLIM. For example, FLIM can be used to monitor intracellular $Ca^{2+}$ concentration via genetically encoded $Ca^{2+}$ indicator (GECI) biosensors (Looger and Griesbeck, 2012; Tian et al., 2012) and small-molecule probes such as $Ca^{2+}$-chelating Oregon Green BAPTA-1 (Kuchibhotla et al., 2009; Lattarulo et al., 2011) (Table 1). Traditionally, FLIM has been considered to be too slow for capturing fast $Ca^{2+}$ changes. However, a parallelized time-correlated single-photon counting (TCSPC) two-photon imaging platform, capable of acquiring an image every 82 ms at 115 µm depth, has been used to monitor $Ca^{2+}$ dynamics by time-lapse 3D FLIM (i.e. 4D FLIM) of a Cerulean–Citrine–troponin-C-based intramolecular FRET biosensor (CerTN L15) expressed in the brain stem of transgenic mice (Radbruch et al., 2015; Rakymzhan et al., 2017; Rinnenthal et al., 2013) (Fig. 2C).

#### Tissue engineering and organoids

FLI and PLIM in tissue engineering frequently deal with 'top-to-bottom' engineering approaches, such as organizing fluidic flow (tissues and organ-on-a-chip) (Perottoni et al., 2021; Zirath et al., 2018; Ahmed et al., 2019), scaffold materials (Appel et al., 2013; Sud et al., 2006; Neto et al., 2020) and, more recently, direct bioprinting of biologics (Ozturk et al., 2016, 2020; Kingsley et al., 2019). Autofluorescence FLIM has been used as a readout parameter to monitor the successful biofabrication of dermal matrix engineered scaffolds (Formigli et al., 2012) and scaffold composition during bioengineered cartilage growth (Fite et al., 2011). $O_2$-sensitive 'biosensor scaffolds' (i.e. tissue engineering scaffolds containing phosphorescent $O_2$-sensing dye) have been employed for the imaging of brain slices, scaffold-colonizing cancer cell aggregates and bone regeneration constructs (Jenkins et al., 2015; Schilling et al., 2019; Trampe et al., 2018; Xue et al., 2013, 2016; Yazgan et al., 2017). Moreover, multiplexed 3D imaging, combining $O_2$ imaging with live-cell labeling, has enabled the tracing of hypoxia-dependent cell differentiation and anticancer drug action (Jenkins et al., 2015). A recent proof-of-concept study has demonstrated that $O_2$-nanosensor-labeled scaffolds can be implanted into mice for long-term monitoring of $O_2$ levels during regeneration and scaffold degradation (Elagin et al., 2020). In addition, such a biosensor scaffold approach allows the sensing of pH, $Ca^{2+}$ and other parameters using 3D FLIM (O'Donnell et al., 2018; Okkelman et al., 2020a).

Organoids and other advanced 'engineered tissue' 3D models permit real-time, quantitative monitoring of genome organization (Lu et al., 2008; Hoppe et al., 2008; Wollman et al., 2020), self-organization of cellular processes (Lu et al., 2008; Hoppe et al., 2008; Wollman et al., 2020), metabolism, intracellular trafficking (Skruzny et al., 2020) and organelle–organelle interactions, as well as cancer cell migration, invasion and metastasis (Alexander et al., 2013; Steuwe et al., 2020), enabling an integrated understanding of the molecular biology of the cell in health and disease. Furthermore, metabolic FLIM and PLIM imaging are valuable tools in developmental biology and research into assisted reproductive technologies (Ma et al., 2019; Sosnik et al., 2016; Stringari et al., 2011, 2012), and hold promise for improving tissue engineering,

recreating stem cell niches and tumor microenvironments and developing advanced tissues-on-a-chip systems (Okkelman et al., 2020b; Ozturk et al., 2020; Floudas et al., 2020; Barron et al., 2020).

#### Contrast enhancement for high-performance 3D imaging and super-resolution microscopy

Luminophores can be distinguished not only by spectra but also by their lifetime values. Thus, multiplexing is a clear advantage of luminescence lifetime imaging, effectively increasing the number of dyes and labels that can be sensed simultaneously in one sample (Fig. 2D). Because the same luminophore can display changes in lifetime via interaction with its immediate environment within the cell, an additional 'contrast' enhancement feature becomes available. In FLI-based approaches, lifetime signatures can be successfully discriminated from unwanted spectrally overlapping autofluorescence signals (Rudkouskaya et al., 2020b; del Rosal and Benayas, 2018; Okkelman et al., 2017b, 2020c; Rich et al., 2013). FLIM as a contrast enhancement methodology has become more popular with the advent of super-resolution microscopy (Auksorius et al., 2008; Bückers et al., 2011; Hell and Wichmann, 1994; Niehörster et al., 2016; Masullo et al., 2020; Thiele et al., 2020), providing a new way to multiplex fluorescence imaging. 3D FLIM for contrast enhancement has been demonstrated in proof-of-concept light-sheet microscopy with optically cleared and fixed samples (Hirvonen et al., 2020; Greger et al., 2011; Favreau et al., 2020; Funane et al., 2018; Mitchell et al., 2017; Weber et al., 2015; Li et al., 2020; Birch et al., 2016).

#### Imaging at the organ or organism level – meso- and macro-scopic luminescence lifetime imaging

FLI can be integrated into a wide range of imaging modalities while retaining the same fundamental physical principles and biological readout information across scales. This is particularly important in the imaging of larger volumes, including tissues, organs and tumors, or in whole-body imaging of small organisms. Here, we will examine FLI-based deep-tissue imaging with mesoscopic (depth of penetration of a few millimeters) and macroscopic (depth of penetration of a few centimeters) optical imaging platforms. In contrast to microscopy, macroscopy involves the visualization of entire volumes (~$mm^3$–$cm^3$) with main applications in whole-body preclinical imaging. Macroscopy can be performed with 2D (reflectance) or 3D (tomography) imaging approaches, both *in vivo* and *ex vivo* (Sinsuebphon et al., 2018; McConnell and Amos, 2018; McConnell et al., 2016; Mizuno et al., 2021). Mesoscopic approaches refer to the scale between microscopic and macroscopic, and include imaging platforms that can visualize whole, intact samples in a size range of 50–100 µm to 2–3 mm. Current mesoscopic imaging applications focus on tissue engineering and/or subsurface preclinical imaging (below the intact skin and/or skull).

Confocal-based macro-FLI implementations collect point-by-point FLI data sets that are processed following the same approach as used in FLIM (Bloch et al., 2005). Macro-FLI confocal scanning platforms provide a larger field of view (of a few $cm^2$, compared to a few hundred $\mu m^2$ in microscopy) with near-cellular resolution FLIM images for the 2D analysis of, for instance, tumor metabolic heterogeneity and fluorescence FRET biosensors (Rinnenthal et al., 2013; Shcheslavskiy et al., 2018; Suhling et al., 2019; Zherdeva et al., 2018) (Fig. 3A). Because they do not account for the effect of light propagation on fluorescence decay, macro-FLI imagers are well suited for imaging of superficial tissues and/or transparent systems, as in both cases scattering is minimal. Macro-FLI imagers have also been used for *ex vivo* whole-organ imaging (Kantelhardt et al., 2016; Papour et al., 2013) and for imaging of the skin in studies of melanoma (Seidenari et al., 2013), pigmentation (Dancik et al., 2013) and wound healing (Rico-Jimenez et al., 2020), as well as to assess nanoparticulate zinc oxide sunscreen safety (Mohammed et al., 2020) and living dermal equivalents (Meleshina et al., 2018).

FLI-based sensing can be combined with other imaging methodological approaches, enabling improved tissue and organ visualization and quantitative analysis. For example, FLI has been integrated with optical coherence tomography (OCT) (Singh et al., 2016), a well-characterized non-invasive imaging approach that provides spatial resolution in the micrometer range by using low-coherence interferometry. Autofluorescence FLI has been merged with high-resolution OCT images to visualize tissue biochemistry and morphology of coronary artery sections (Sherlock et al., 2017; Shrestha et al., 2016) (Fig. 3B). OCT–FLIM has also been used in cancer diagnosis (Lee et al., 2018; Nam et al., 2018; Pande et al., 2016), as well as in the characterization of atherosclerotic plaques (Lee et al., 2018; Nam et al., 2018; Pande et al., 2016). In addition, FLI imaging has been enhanced through integration with OPT (Andrews et al., 2016; McGinty et al., 2011) (Fig. 3C), a form of tomography involving optical microscopy (Sharpe et al., 2002), ultrasound (Bec et al., 2014) or spatial frequency domain imaging (Smith et al., 2020a), a widefield diffuse optical imaging technique that can be used to obtain absorption and reduced scattering coefficients of turbid media (Gioux et al., 2019). Whereas these applications focus on shallow tissues and rely on the same principle as FLIM for image formation, for the imaging of deeper tissues, more complex mathematical formulations that take into account the optical tissue properties are required.

To perform imaging of deeper tissues, methodologies such as minimally invasive endoscopy or FMT need to be employed (Box 1). Deep-tissue imaging also requires the use of near-infrared (NIR) dyes, as tissue attenuation is reduced in the NIR optical window and autofluorescence is drastically decreased (Staudinger and Borisov, 2015). Moreover, macroscopic deeper imaging approaches are suitable for non-invasive imaging, allowing for imaging across the intact skin, which maintains the undisrupted native physiology and environment of organs and tissues, albeit at the cost of resolution. The flexibility of FLI has allowed its use in endoscopy for multiple *in vivo* applications via a fiber-optic bundle (Duran-Sierra et al., 2020; Hage et al., 2019; Jo et al., 2018; Won et al., 2016). FMT is a non-invasive and non-ionizing optical imaging modality that retrieves the biomarkers of interest in 3D volumes. It is based on acquiring optical data from spatially resolved surface measurements and performing mathematical computational tasks that involve the modeling of light propagation according to tissue scattering properties. Briefly, a forward model of light propagation is computed for every spatially resolved measurement acquired from the imaging system (Arridge, 1999) and then compared iteratively with the experimental data to yield 3D digitized maps of intensity contrasts (Chen et al., 2012). This mathematical task is referred to as an inverse problem and it is at the basis of image formation in numerous 3D imaging modalities, including computed tomography (CT) and nuclear imaging. In the case of FMT, the goal is to determine the 3D biodistribution of NIR dyes in deep organs, such as the liver, lungs and brain, or orthotopic tumor xenografts. Different tomographic imaging approaches have used FLI contrast to visualize and quantify gene function and protein expression in a variety of organs by using whole-body non-invasive imaging of genetically encoded NIR-fluorescent proteins or NIR-labeled nanoparticles (Cai et al., 2016; Kumar et al., 2018;

Rice et al., 2015), as well as NIR-labeled antibody or ligand probes (Cai et al., 2016; Kumar et al., 2018; Nothdurft et al., 2009; Rice et al., 2015) (Fig. 3D). FLI–FRET tomographic reconstructions of deep-seated organs can provide nanoscale sensing in deep tissue, in the millimeter range, enabling the imaging of whole organs or even small animals (Box 1). To that end, volumetric imaging of genetically expressed fluorescent proteins (McGinty et al., 2011) or NIR-labeled probes (Venugopal et al., 2012) has already been obtained using FLI-based tomographic reconstruction of FRET measurements (Fig. 3E,F). One very promising application for these emerging FLI–FRET whole-body imaging systems is the monitoring of the intracellular delivery of targeted probes in live animals by quantifying the ligand–receptor efficiency across organs. For example, FMT has been used in conjunction with structured light illumination to achieve quantitative 3D FRET tomographic non-invasive *in vivo* macroscopic FLI (MFLI) imaging of subcutaneous tumor xenografts to measure drug delivery (Rudkouskaya et al., 2018, 2020b). Subsequently, *in vivo* multiplexed MFLI–FRET imaging of receptor–ligand target engagement and glucose metabolism in tumor xenografts in live intact animals has been demonstrated (Rudkouskaya et al., 2020a). However, tomographic image reconstructions are computationally expensive and require expertise in light propagation modeling, limiting their use in biomedical applications (Leblond et al., 2010). Hence, there is a growing interest in developing fit-free FLI analysis, such as phasor (Chen et al., 2019; Ma et al., 2019) and deep learning (Smith et al., 2019; Ochoa et al., 2020) methodologies. Considering the plethora of FLIM-based approaches for imaging 2D oncologic samples, and their many applications (Ardeshirpour et al., 2018; Basuki et al., 2013; Mehidine et al., 2019; Pal et al., 2019; Sparks et al., 2018; Weitsman et al., 2017), further advancing the ability to perform macroscopic FLI and tomographic reconstructions of deep-seated tumors in their native and undisrupted environment has the potential to accelerate cancer drug screening and efficacy assessment, as well as tumor biology research.

#### FLIM for live subcellular imaging in 3D

Advances in structured plane illumination and super-resolution microscopy have increased the appreciation for the complexity of subcellular organelle morphology and dynamics in 3D (Liu et al., 2018a). Thus, by enabling a functional *in situ* and live readout from these complex structures, FLIM is particularly suited to the study of chromatin compaction, subnuclear organization (Angelier et al., 2005; Wollman et al., 2020; Cremazy et al., 2005; Rino and Carmo-Fonseca, 2009), cell membrane-anchored processes, organelle biogenesis and other subcellular processes. For instance, FLIM–FRET has been used to monitor the heterochromatin organization in live *Caenorhabditis elegans* (Llères et al., 2017), and 3D FLIM was employed to study chromatin compaction in response to DNA damage using histone H2B–fluorescent protein fusion probes (Sherrard et al., 2018). In addition, a phasor-based approach to FLIM–FRET analysis of chromatin compaction has been described (Lou et al., 2019). DNA-staining dyes and fluorescent protein reporters have also been used for FLIM analysis of events in the nucleus (Abdollahi et al., 2018; Audugé et al., 2019; Estandarte et al., 2016; Kawanabe et al., 2015; Okkelman et al., 2016; Sparks et al., 2018).

The interactions of luminescent dyes with biomolecules, resulting in changes in their aggregation state, molecular rotation and lifetime values, have been extensively employed to study membrane composition by FLIM using probes, such as C6-NBD-PC and Laurdan, and viscosity-sensitive fluorescent molecular rotors (Kuimova, 2012; Levitt et al., 2015; Ringer et al., 2017; Stöckl et al., 2012). Use of these probes has enabled a deeper understanding of cell cycle-dependent changes in membrane composition (Denz et al., 2017) and of lipid bilayer organization with regard to rafts and microdomains (Carquin et al., 2016; Ma et al., 2018; Malacrida and Gratton, 2018). Recently, FLIM–FRET has been used to provide mechanistic insight into lipid and protein interaction sites between the endoplasmic reticulum and the trans-Golgi network (Venditti et al., 2019). Furthermore, 3D FLIM–FRET has allowed for the analysis of viscosity in tumor spheroids (Shirmanova et al., 2017) and lipid droplets in intestinal organoids (Okkelman et al., 2020a).

## Emerging developments and application areas

The main current bottlenecks of FLI are associated with software optimization, standardization of functional assays and overall cost. For example, one of the classical limitations of FLIM is in the ability to quantify fluorescence lifetimes in low photon budget conditions, such as those encountered in biomedical microscopy applications. This has been typically addressed by the use of iterative algorithms that necessitate user inputs and can be computationally expensive. Recent innovations in phasor plot analysis (Zhang et al., 2019; Vallmitjana et al., 2020) represent attractive alternatives given their speed, user friendliness and potential for standardization. To highlight this, we provide below two examples of emerging 3D FLI developments.

#### Machine learning for FLI

To date, leveraging of new developments in artificial intelligence has mainly been performed for classification and segmentation of raw FLI data (Mannam et al., 2020) using classical supervised machine learning algorithmic techniques, such as support vector machines (SVM) (Zhang et al., 2019), k-means clustering (Brodwolf et al., 2020; Zhang et al., 2019), or ‘random forest’ machine learning algorithms (Walsh et al., 2020). However, deep learning, another class of artificial intelligence algorithms, is well known to outperform such ‘shallow learning’ classifiers by, for example, forming the FLI image directly from raw data, and deep learning methods are expected to become the norm for such image-processing tasks. Moreover, deep learning approaches are well suited to tackle the mathematical inverse problem associated with lifetime quantification. This has been demonstrated in a recent study that proposed a deep learning model, named FLI-Net, that is user-input free, processes whole images almost in real time and, of great importance to biological applications, is more accurate in low photon budget conditions than current ubiquitous techniques (Smith et al., 2019). Moreover, deep learning methodologies have been used to enhance unmixing approaches for increased specificity (Smith et al., 2020b). Lastly, they can facilitate the implementation of the next generation of high-end FLI instruments, especially hyperspectral macroscopic FLI systems (Pian et al., 2017; Yao et al., 2019; Ochoa et al., 2020). Hence, deep learning methods are expected to play a crucial role in the increased utilization of 3D, spectral and time-lapse reconstruction of live multiparameter sets of FLI, FLIM and PLIM data in biomedical imaging applications.

#### FLI for viral and pathogen research

Viral and pathogen infection of mammalian cells result in changes to membrane composition. In addition, virus replication and capsid assembly are highly demanding for cellular bioenergetics and metabolism. Therefore, viral research is an attractive application for

FLI, FLIM and PLIM approaches. Unsurprisingly, FLIM has been extensively used to characterize human immunodeficiency virus 1 (HIV-1) infection, including capsid assembly and viral particle trafficking to the plasma membrane, as well as its dependence on cell metabolism and cholesterol content (Jones and Padilla-Parra, 2015; Coomer et al., 2020; de Rocquigny et al., 2014; El Meshri et al., 2015; Greiner et al., 2011). Other FLIM studies have investigated the assembly of influenza virus capsids (Thaa et al., 2010), adenovirus type-5 entry and disassembly (Martin-Fernandez et al., 2004), enterovirus 71 entry into cells (Ghukasyan et al., 2007), the effects of enterohemorrhagic *Escherichia coli* infection (Buryakina et al., 2012), and leaf chlorosis due to plant virus infection (Lei et al., 2017). These studies have mostly made use of single-cell FLIM imaging approaches (Witte et al., 2018). However, they could clearly benefit from being combined with more physiologically relevant 3D tissue organoid models. Moreover, the use of highly efficient tools to track viruses in live and physiological settings (Clevers, 2020) would improve and further streamline antiviral research and the development of therapeutics. Thus, FLI and PLIM methodologies are not restricted to animal cell and tissue imaging and can be used more widely, beyond biomedical applications, to include imaging-based research of other classes and kingdoms of life (Box 2).

### Box 2. FLI(M) in aquatic organisms, photosynthetic organisms, biofilms and fungi

The fields of aquatic and plant biology research, among others, also benefit from 3D FLIM (Moßhammer et al., 2019). For instance, $O_2$ imaging using various nanoparticles is useful for the study of corals and plant-based inter-species systems such as those that exist in the rhizosphere (Fabricius-Dyg et al., 2012; Brodersen et al., 2020). Similar to NAD(P)H sensing in biomedical imaging, chlorophyll autofluorescence FLIM can be used to analyse the metabolic function of coral symbionts. Unfortunately, only a few research studies have attempted to investigate this (Cox et al., 2007; Petrášek et al., 2009; Shapiro et al., 2016).

Although the leaves of terrestrial plants and their photosynthetic pigments were among the first biological systems to be imaged using autofluorescence FLIM (Donaldson, 2020; García-Plazaola et al., 2015; Holub et al., 2000; Oxborough and Baker, 1997), the technique is rarely used in plant sciences and photosynthesis research (Cisek et al., 2009; Emiliani et al., 2003; Iermak et al., 2016). Plant seeds (including barley embryos) have been studied using autofluorescence imaging, with two-photon FLIM multiplexed with magnetic resonance imaging (Stark et al., 2007) being applied to distinguish between functionally different parts of the seed, specifically the seed coat, embryo and starch. FLIM–FRET has also been used to monitor protein interactions using overexpressed biosensors in another kingdom of life, the fungi (Altenbach et al., 2009).

Bacterial biofilms, which play highly important barrier and transport functions in microbial communities, represent another interesting application for 3D FLIM (Schlafer and Meyer, 2017). Biofilms often grow as 3D structures, and understanding their function is of high importance for basic biology, environmental science and biomedicine, for example in host–microbe interactions and in dental and human skin microbiome research (Brandwein et al., 2016; Hatzenpichler et al., 2020; Soll and Daniels, 2016). Until now, FLIM of biofilms has been focused on introducing staining dyes to map extracellular pH and FRET-based measurements (Schlafer and Meyer, 2017), as well as labeling and visualizing DNA and RNA using two-photon FLIM (Neu et al., 2004). *In situ* FLIM imaging using the dye SYTO 13 to measure DNA:RNA ratio has allowed the visualization of different bacterial communities within the same biofilm (Walczysko et al., 2008). Among the important components of the biofilm matrixome, the dynamics of $O_2$ has been assessed using spinning-disk FLIM (Kühl et al., 2007).

## Conclusions

Luminescence lifetime imaging, as it becomes more available to researchers of varying expertise, enables a redefinition of classic fluorescence imaging, thus opening a new avenue for the use of dyes and biosensor probes (making virtually any dye a biosensor) and producing a new, 'molecular' dimension in a wide variety of imaging platforms. Although it can easily provide additional benefits to imaging modalities that utilize dead, fixed or optically cleared tissues (for example by improving quality, resolution and the effective number of used fluorophores in super-resolution microscopy), its main power and potential to be harnessed in the coming decade lies in advanced live imaging of complex 3D objects, including studying virus infection in engineered 'niches', tissues, tissue organoids and small organisms.

#### Acknowledgements

We would like to thank the members of the Barroso, Intes and Dmitriev laboratories for comments and discussions that are at the basis of this Review. In particular, we would like to thank Dr Jonathan Barra for his careful and detailed review of the manuscript.

#### Competing interests

The authors declare no competing or financial interests.

#### Funding

Our research in this area is funded by grants from the National Institutes of Health (R01 CA250636, R01 CA207725 and R01 CA237267 to M.M.B. and X.I.) and Universiteit Gent (BOF/STA/202009/003 to R.I.D.). Deposited in PMC for release after 12 months.

#### References

**Abdollahi, E., Taucher-Scholz, G. and Jakob, B.** (2018). Application of fluorescence lifetime imaging microscopy of DNA binding dyes to assess radiation-induced chromatin compaction changes. *Int. J. Mol. Sci.* **19**, 2399. doi:10.3390/ijms19082399

**Abe, K., Zhao, L., Periasamy, A., Intes, X. and Barroso, M.** (2013). Non-invasive in vivo imaging of near infrared-labeled transferrin in breast cancer cells and tumors using fluorescence lifetime FRET. *PLoS ONE* **8**, e80269. doi:10.1371/journal.pone.0080269

**Ahmed, S., Chauhan, V. M., Ghaemmaghami, A. M. and Aylott, J. W.** (2019). New generation of bioreactors that advance extracellular matrix modelling and tissue engineering. *Biotechnol. Lett.* **41**, 1-25. doi:10.1007/s10529-018-2611-7

**Alam, S. R., Wallrabe, H., Svindrych, Z., Chaudhary, A. K., Christopher, K. G., Chandra, D. and Periasamy, A.** (2017). Investigation of mitochondrial metabolic response to doxorubicin in prostate cancer cells: an Nadh, FAD and tryptophan FLIM assay. *Sci. Rep.* **7**, 1-10.

**Alexander, S., Weigelin, B., Winkler, F. and Friedl, P.** (2013). Preclinical intravital microscopy of the tumour-stroma interface: invasion, metastasis, and therapy response. *Curr. Opin. Cell Biol.* **25**, 659-671. doi:10.1016/j.ceb.2013.07.001

**Altenbach, K., Duncan, R. R. and Valkonen, M.** (2009). In vivo FLIM-FRET measurements of recombinant proteins expressed in filamentous fungi. *Fungal Biol. Rev.* **23**, 67-71. doi:10.1016/j.fbr.2009.12.002

**Amaro, M., Šachl, R., Jurkiewicz, P., Coutinho, A., Prieto, M. and Hof, M.** (2014). Time-resolved fluorescence in lipid bilayers: selected applications and advantages over steady state. *Biophys. J.* **107**, 2751-2760. doi:10.1016/j.bpj.2014.10.058

**Andrews, N., Ramel, M. C., Kumar, S., Alexandrov, Y., Kelly, D. J., Warren, S. C., Kerry, L., Lockwood, N., Frolov, A., Frankel, P. et al.** (2016). Visualising apoptosis in live zebrafish using fluorescence lifetime imaging with optical projection tomography to map FRET biosensor activity in space and time. *J. Biophoton.* **9**, 414-424. doi:10.1002/jbio.201500258

**Angelier, N., Tramier, M., Louvet, E., Coppey-Moisan, M., Savino, T. M., De Mey, J. R. and Hernandez-Verdun, D.** (2005). Tracking the interactions of rRNA processing proteins during nucleolar assembly in living cells. *Mol. Biol. Cell* **16**, 2862-2871. doi:10.1091/mbc.e05-01-0041

**Appel, A. A., Anastasio, M. A., Larson, J. C. and Brey, E. M.** (2013). Imaging challenges in biomaterials and tissue engineering. *Biomaterials* **34**, 6615-6630. doi:10.1016/j.biomaterials.2013.05.033

**Ardeshirpour, Y., Sackett, D. L., Knutson, J. R. and Gandjbakhche, A. H.** (2018). Using in vivo fluorescence lifetime imaging to detect HER2-positive tumors. *EJNMMI Res.* **8**, 26. doi:10.1186/s13550-018-0384-6

**Arridge, S. R.** (1999). Optical tomography in medical imaging. *Inverse Probl.* **15**, R41. doi:10.1088/0266-5611/15/2/022

**Audugé, N., Padilla-Parra, S., Tramier, M., Borghi, N. and Coppey-Moisan, M.** (2019). Chromatin condensation fluctuations rather than steady-state predict chromatin accessibility. *Nucleic Acids Res.* **47**, 6184-6194. doi:10.1093/nar/gkz373

**Auksorius, E., Boruah, B. R., Dunsby, C., Lanigan, P. M. P., Kennedy, G., Neil, M. A. A. and French, P. M. W.** (2008). Stimulated emission depletion microscopy with a supercontinuum source and fluorescence lifetime imaging. *Opt. Lett.* **33**, 113-115. doi:10.1364/OL.33.000113

**Bakker, G.-J., Andresen, V., Hoffman, R. M. and Friedl, P.** (2012). Fluorescence lifetime microscopy of tumor cell invasion, drug delivery, and cytotoxicity. *Methods Enzymol.* **504**, 109-125. doi:10.1016/B978-0-12-391857-4.00005-7

**Barlow, C. H. and Chance, B.** (1976). Ischemic areas in perfused rat hearts: measurement by NADH fluorescence photography. *Science* **193**, 909-910. doi:10.1126/science.181843

**Barron, M. R., Cieza, R. J., Hill, D. R., Huang, S., Yadagiri, V. K., Spence, J. R. and Young, V. B.** (2020). The Lumen of Human Intestinal Organoids Poses Greater Stress to Bacteria Compared to the Germ-Free Mouse Intestine: Escherichia coli Deficient in RpoS as a Colonization Probe. *mSphere* **5**, e00777-20. doi:10.1128/mSphere.00777-20

**Basuki, J. S., Duong, H. T. T., Macmillan, A., Erlich, R. B., Esser, L., Akerfeldt, M. C., Whan, R. M., Kavallaris, M., Boyer, C. and Davis, T. P.** (2013). Using fluorescence lifetime imaging microscopy to monitor theranostic nanoparticle uptake and intracellular doxorubicin release. *ACS Nano* **7**, 10175-10189. doi:10.1021/nn404407g

**Bec, J., Ma, D. M., Yankelevich, D. R., Liu, J., Ferrier, W. T., Southard, J. and Marcu, L.** (2014). Multispectral fluorescence lifetime imaging system for intravascular diagnostics with ultrasound guidance: in vivo validation in swine arteries. *J. Biophoton.* **7**, 281-285. doi:10.1002/jbio.201200220

**Becker, W., Shcheslavskiy, V. and Rück, A.** (2017). Simultaneous phosphorescence and fluorescence lifetime imaging by multi-dimensional TCSPC and multi-pulse excitation. *Multi-Parametric Live Cell Microsc. 3D Tissue Model.* **1035**, 19-30. doi:10.1007/978-3-319-67358-5_2

**Berezin, M. Y. and Achilefu, S.** (2010). Fluorescence lifetime measurements and biological imaging. *Chem. Rev.* **110**, 2641-2684. doi:10.1021/cr900343z

**Birch, P. M., Moore, L, Li, X., Phillips, R., Young, R. and Chatwin, C.** (2016). A wide field fluorescence lifetime imaging system using a light sheet microscope. In Biophotonics: Photonic Solutions for Better Health Care V. International Society for Optics and Photonics. Vol. 9887. Brussels: SPIE Photonics Europe. doi:10.1117/12.2230908

**Blacker, T. S. and Duchen, M. R.** (2016). Investigating mitochondrial redox state using NADH and NADPH autofluorescence. *Free Radic. Biol. Med.* **100**, 53-65. doi:10.1016/j.freeradbiomed.2016.08.010

**Blacker, T. S., Mann, Z. F., Gale, J. E., Ziegler, M., Bain, A. J., Szabadkai, G. and Duchen, M. R.** (2014). Separating NADH and NADPH fluorescence in live cells and tissues using FLIM. *Nat. Commun.* **5**, 3936. doi:10.1038/ncomms4936

**Bloch, S., Lesage, F., Mcintosh, L., Gandjbakhche, A., Liang, K. and Achilefu, S.** (2005). Whole-body fluorescence lifetime imaging of a tumor-targeted near-infrared molecular probe in mice. *J. Biomed. Opt.* **10**, 054003. doi:10.1117/1.2070148

**Brand, M. D. and Nicholls, D. G.** (2011). Assessing mitochondrial dysfunction in cells. *Biochem. J.* **435**, 297-312. doi:10.1042/BJ20110162

**Brandwein, M., Steinberg, D. and Meshner, S.** (2016). Microbial biofilms and the human skin microbiome. *NPJ Biofilm. Microbiomes* **2**, 3. doi:10.1038/s41522-016-0004-z

**Brodersen, K. E., Kühl, M., Trampe, E. and Koren, K.** (2020). Imaging O2 dynamics and microenvironments in the seagrass leaf phyllosphere with magnetic optical sensor nanoparticles. *Plant J.* **104**, 1504-–1519. doi:10.1111/tpj.15017

**Brodwolf, R., Volz-Rakebrand, P., Stellmacher, J., Wolff, C., Unbehauen, M., Haag, R., Schäfer-Korting, M., Zoschke, C. and Alexiev, U.** (2020). Faster, sharper, more precise: Automated Cluster-FLIM in preclinical testing directly identifies the intracellular fate of theranostics in live cells and tissue. *Theranostics* **10**, 6322. doi:10.7150/thno.42581

**Bückers, J., Wildanger, D., Vicidomini, G., Kastrup, L. and Hell, S. W.** (2011). Simultaneous multi-lifetime multi-color STED imaging for colocalization analyses. *Opt. Express* **19**, 3130-3143. doi:10.1364/OE.19.003130

**Bunt, G. and Wouters, F. S.** (2017). FRET from single to multiplexed signaling events. *Biophys. Rev.* **9**, 119-129. doi:10.1007/s12551-017-0252-z

**Buryakina, T., Su, P.-T., Syu, W.-J., Chang, C. A., Fan, H.-F. and Kao, F.-J.** (2012). Metabolism of HeLa cells revealed through autofluorescence lifetime upon infection with enterohemorrhagic Escherichia coli. *J. Biomed. Opt.* **17**, 101503. doi:10.1117/1.JBO.17.10.101503

**Cai, C., Cai, W., Cheng, J., Yang, Y. and Luo, J.** (2016). Self-guided reconstruction for time-domain fluorescence molecular lifetime tomography. *J. Biomed. Opt.* **21**, 126012. doi:10.1117/1.JBO.21.12.126012

**Carquin, M., D'auria, L., Pollet, H., Bongarzone, E. R. and Tyteca, D.** (2016). Recent progress on lipid lateral heterogeneity in plasma membranes: from rafts to submicrometric domains. *Prog. Lipid Res.* **62**, 1-24. doi:10.1016/j.plipres.2015.12.004

**Chen, J., Fang, Q. and Intes, X.** (2012). Mesh-based Monte Carlo method in time-domain widefield fluorescence molecular tomography. *J. Biomed. Opt.* **17**, 106009. doi:10.1117/1.JBO.17.10.106009

**Chen, S.-J., Sinsuebphon, N., Rudkouskaya, A., Barroso, M., Intes, X. and Michalet, X.** (2019). In vitro and in vivo phasor analysis of stoichiometry and pharmacokinetics using short-lifetime near-infrared dyes and time-gated imaging. *J. Biophotonics* **12**, e201800185. doi:10.1002/jbio.201800185

**Cheng, X., Sadegh, S., Zilpelwar, S., Devor, A., Tian, L. and Boas, D. A.** (2020). Comparing the fundamental imaging depth limit of two-photon, three-photon, and non-degenerate two-photon microscopy. *Opt. Lett.* **45**, 2934-2937. doi:10.1364/OL.392724

**Chennell, G., Willows, R. J., Warren, S. C., Carling, D., French, P. M., Dunsby, C. and Sardini, A.** (2016). Imaging of metabolic status in 3D cultures with an improved AMPK FRET biosensor for FLIM. *Sensors* **16**, 1312. doi:10.3390/s16081312

**Chrétien, D., Bénit, P., Ha, H.-H., Keipert, S., El-Khoury, R., Chang, Y.-T., Jastroch, M., Jacobs, H. T., Rustin, P. and Rak, M.** (2018). Mitochondria are physiologically maintained at close to 50 C. *PLoS Biol.* **16**, e2003992. doi:10.1371/journal.pbio.2003992

**Christodoulou, C., Spencer, J. A., Yeh, S.-C. A., Turcotte, R., Kokkaliaris, K. D., Panero, R., Ramos, A., Guo, G., Seyedhassantehrani, N., Esipova, T. V. et al.** (2020). Live-animal imaging of native haematopoietic stem and progenitor cells. *Nature* **578**, 278-283. doi:10.1038/s41586-020-1971-z

**Cisek, R., Spencer, L., Prent, N., Zigmantas, D., Espie, G. S. and Barzda, V.** (2009). Optical microscopy in photosynthesis. *Photosynth. Res.* **102**, 111-141. doi:10.1007/s11120-009-9500-9

**Clevers, H.** (2020). COVID-19: organoids go viral. *Nat. Rev. Mol. Cell Biol.* **21**, 355-356. doi:10.1038/s41580-020-0258-4

**Conway, J. R. W., Warren, S. C. and Timpson, P.** (2017). Context-dependent intravital imaging of therapeutic response using intramolecular FRET biosensors. *Methods* **128**, 78-94. doi:10.1016/j.ymeth.2017.04.014

**Conway, J. R. W., Warren, S. C., Herrmann, D., Murphy, K. J., Cazet, A. S., Vennin, C., Shearer, R. F., Killen, M. J., Magenau, A., Mélénec, P. et al.** (2018). Intravital imaging to monitor therapeutic response in moving hypoxic regions resistant to PI3K pathway targeting in pancreatic cancer. *Cell Rep.* **23**, 3312-3326. doi:10.1016/j.celrep.2018.05.038

**Coomer, C. A., Carlon-Andres, I., Iliopoulou, M., Dustin, M. L., Compeer, E. B., Compton, A. A. and Padilla-Parra, S.** (2020). Single-cell glycolytic activity regulates membrane tension and HIV-1 fusion. *PLoS Pathog.* **16**, e1008359. doi:10.1371/journal.ppat.1008359

**Cox, G., Matz, M. and Salih, A.** (2007). Fluorescence lifetime imaging of coral fluorescent proteins. *Microsc. Res. Tech.* **70**, 243-251. doi:10.1002/jemt.20410

**Cremazy, F. G., Manders, E. M., Bastiaens, P. I., Kramer, G., Hager, G. L., van Munster, E. B., Verschure, P. J., Gadella, T. J., Jr and van Driel, R.** (2005). Imaging in situ protein–DNA interactions in the cell nucleus using FRET–FLIM. *Exp. Cell Res.* **309**, 390-396. doi:10.1016/j.yexcr.2005.06.007

**Dancik, Y., Favre, A., Loy, C. J., Zvyagin, A. V. and Roberts, M. S.** (2013). Use of multiphoton tomography and fluorescence lifetime imaging to investigate skin pigmentation in vivo. *J. Biomed. Opt.* **18**, 026022. doi:10.1117/1.JBO.18.2.026022

**Datta, R., Heaster, T. M., Sharick, J. T., Gillette, A. A. and Skala, M. C.** (2020). Fluorescence lifetime imaging microscopy: fundamentals and advances in instrumentation, analysis, and applications. *J. Biomed. Opt.* **25**, 071203. doi:10.1117/1.JBO.25.7.071203

**de Rocquigny, H., el Meshri, S. E., Richert, L., Didier, P., Darlix, J.-L. and Mély, Y.** (2014). Role of the nucleocapsid region in HIV-1 Gag assembly as investigated by quantitative fluorescence-based microscopy. *Virus Res.* **193**, 78-88. doi:10.1016/j.virusres.2014.06.009

**del Rosal, B. and Benayas, A.** (2018). Strategies to overcome autofluorescence in nanoprobe-driven in vivo fluorescence imaging. *Small Methods* **2**, 1800075. doi:10.1002/smtd.201800075

**Denicke, S., Ehlers, J.-E., Niesner, R., Quentmeier, S. and Gericke, K.-H.** (2007). Steady-state and time-resolved two-photon fluorescence microscopy: a versatile tool for probing cellular environment and function. *Phys. Scr.* **76**, C115. doi:10.1088/0031-8949/76/3/N18

**Denz, M., Chiantia, S., Herrmann, A., Mueller, P., Korte, T. and Schwarzer, R.** (2017). Cell cycle dependent changes in the plasma membrane organization of mammalian cells. *Biochim. Biophys. Acta Biomembr.* **1859**, 350-359. doi:10.1016/j.bbamem.2016.12.004

**Devor, A., Sakadžić, S., Srinivasan, V. J., Yaseen, M. A., Nizar, K., Saisan, P. A., Tian, P., Dale, A. M., Vinogradov, S. A., Franceschini, M. A. et al.** (2012). Frontiers in optical imaging of cerebral blood flow and metabolism. *J. Cereb. Blood Flow Metab.* **32**, 1259-1276. doi:10.1038/jcbfm.2011.195

**Díaz-García, C. M., Lahmann, C., Martínez-François, J. R., Li, B., Koveal, D., Nathwani, N., Rahman, M., Keller, J. P., Marvin, J. S., Looger, L. L. et al.** (2019). Quantitative in vivo imaging of neuronal glucose concentrations with a genetically encoded fluorescence lifetime sensor. *J. Neurosci. Res.* **97**, 946-960. doi:10.1002/jnr.24433

**Digman, M. A., Caiolfa, V. R., Zamai, M. and Gratton, E.** (2008). The phasor approach to fluorescence lifetime imaging analysis. *Biophys. J.* **94**, L14-L16. doi:10.1529/biophysj.107.120154

**Dmitriev, R. I.** (ed.). (2017). *Multi-Parametric Live Cell Microscopy of 3D Tissue Models*. Springer International Publishing AG 2017.

**Dmitriev, R. I. and Papkovsky, D. B.** (2012). Optical probes and techniques for O2 measurement in live cells and tissue. *Cell. Mol. Life Sci.* **69**, 2025-2039. doi:10.1007/s00018-011-0914-0

**Dmitriev, R. I. and Papkovsky, D. B.** (2015). Intracellular probes for imaging oxygen concentration: How good are they? *Methods Appl. Fluorescence* **3**, 034001. doi:10.1088/2050-6120/3/3/034001

**Dmitriev, R. I., Zhdanov, A. V., Jasionek, G. and Papkovsky, D. B.** (2012). Assessment of cellular oxygen gradients with a panel of phosphorescent oxygen-sensitive probes. *Anal. Chem.* **84**, 2930-2938. doi:10.1021/ac3000144

**Dmitriev, R. I., Zhdanov, A. V., Nolan, Y. M. and Papkovsky, D. B.** (2013). Imaging of neurosphere oxygenation with phosphorescent probes. *Biomaterials* **34**, 9307-9317. doi:10.1016/j.biomaterials.2013.08.065

**Dmitriev, R. I., Kondrashina, A. V., Koren, K., Klimant, I., Zhdanov, A. V., Pakan, J. M. P., Mcdermott, K. W. and Papkovsky, D. B.** (2014). Small molecule phosphorescent probes for $O_2$ imaging in 3D tissue models. *Biomater. Sci.* **2**, 853-866. doi:10.1039/C3BM60272A

**Dmitriev, R. I., Borisov, S. M., Düssmann, H., Sun, S., Müller, B. J., Prehn, J., Baklaushev, V. P., Klimant, I. and Papkovsky, D. B.** (2015a). Versatile conjugated polymer nanoparticles for high-resolution $O_2$ imaging in cells and 3D tissue models. *ACS Nano* **9**, 5275-5288. doi:10.1021/acsnano.5b00771

**Dmitriev, R. I., Borisov, S. M., Jenkins, J. and Papkovsky, D. B.** (2015b). Multi-parametric imaging of tumor spheroids with ultra-bright and tunable nanoparticle $O_2$ probes. *Photonics West* **2015**, 932806. doi:10.1117/12.2079604

**Donaldson, L.** (2020). Autofluorescence in Plants. *Molecules* **25**, 2393. doi:10.3390/molecules25102393

**Dumas, J.-P., Jiang, J. Y., Gates, E. M., Hoffman, B. D., Pierce, M. C. and Boustany, N. N.** (2019). FRET efficiency measurement in a molecular tension probe with a low-cost frequency-domain fluorescence lifetime imaging microscope. *J. Biomed. Opt.* **24**, 126501. doi:10.1117/1.JBO.24.12.126501

**Duran-Sierra, E., Cheng, S., Cuenca-Martinez, R., Malik, B., Maitland, K. C., Cheng, Y. L., Wright, J., Ahmed, B., Ji, J., Martinez, M. et al.** (2020). Clinical label-free biochemical and metabolic fluorescence lifetime endoscopic imaging of precancerous and cancerous oral lesions. *Oral Oncol.* **105**, 104635. doi:10.1016/j.oraloncology.2020.104635

**El Meshri, S. E., Dujardin, D., Godet, J., Richert, L., Boudier, C., Darlix, J. L., Didier, P., Mély, Y. and de Rocquigny, H.** (2015). Role of the nucleocapsid domain in HIV-1 Gag oligomerization and trafficking to the plasma membrane: a fluorescence lifetime imaging microscopy investigation. *J. Mol. Biol.* **427**, 1480-1494. doi:10.1016/j.jmb.2015.01.015

**Elagin, V., Kuznetsova, D., Grebenik, E., Zolotov, D. A., Istranov, L., Zharikova, T., Istranova, E., Polozova, A., Reunov, D., Kurkov, A. et al.** (2020). Multiparametric optical bioimaging reveals the fate of epoxy crosslinked biomeshes in the mouse subcutaneous implantation model. *Front. Bioeng. Biotechnol.* **8**. fbioe.2020.00107. doi:10.3389/fbioe.2020.00107

**Ellenbroek, S. I. J. and van Rheenen, J.** (2014). Imaging hallmarks of cancer in living mice. *Nat. Rev. Cancer* **14**, 406-418. doi:10.1038/nrc3742

**Emiliani, V., Sanvitto, D., Tramier, M., Piolot, T., Petrasek, Z., Kemnitz, K., Durieux, C. and Coppey-Moisan, M.** (2003). Low-intensity two-dimensional imaging of fluorescence lifetimes in living cells. *Appl. Phys. Lett.* **83**, 2471-2473. doi:10.1063/1.1604938

**Esipova, T. V., Barrett, M. J. P., Erlebach, E., Masunov, A. E., Weber, B. and Vinogradov, S. A.** (2019). Oxyphor 2P: a high-performance probe for deep-tissue longitudinal oxygen imaging. *Cell Metab.* **29**, 736-744.e7. doi:10.1016/j.cmet.2018.12.022

**Estandarte, A. K., Botchway, S., Lynch, C., Yusuf, M. and Robinson, I.** (2016). The use of DAPI fluorescence lifetime imaging for investigating chromatin condensation in human chromosomes. *Sci. Rep.* **6**, 31417. doi:10.1038/srep31417

**Fabricius-Dyg, J., Mistlberger, G., Staal, M., Borisov, S. M., Klimant, I. and Kühl, M.** (2012). Imaging of surface O2 dynamics in corals with magnetic micro optode particles. *Mar. Biol.* **159**, 1621-1631. doi:10.1007/s00227-012-1920-y

**Favreau, P. F., He, J., Gil, D. A., Deming, D. A., Huisken, J. and Skala, M. C.** (2020). Label-free redox imaging of patient-derived organoids using selective plane illumination microscopy. *Biomed. Optics Express* **11**, 2591-2606. doi:10.1364/BOE.389164

**Finikova, O. S., Lebedev, A. Y., Aprelev, A., Troxler, T., Gao, F., Garnacho, C., Muro, S., Hochstrasser, R. M. and Vinogradov, S. A.** (2008). Oxygen microscopy by two-photon-excited phosphorescence. *Chemphyschem* **9**, 1673-1679. doi:10.1002/cphc.200800296

**Fite, B. Z., Decaris, M., Sun, Y., Sun, Y., Lam, A., Ho, C. K. L., Leach, J. K. and Marcu, L.** (2011). Noninvasive multimodal evaluation of bioengineered cartilage constructs combining time-resolved fluorescence and ultrasound imaging. *Tissue Eng Part C Methods* **17**, 495-504. doi:10.1089/ten.tec.2010.0368

**Floudas, A., Neto, N., Marzaioli, V., Murray, K., Moran, B., Monaghan, M. G., Low, C., Mullan, R. H., Rao, N., Krishna, V. et al.** (2020). Pathogenic, glycolytic PD-1+ B cells accumulate in the hypoxic RA joint. *JCI Insight* **5**, 1894. doi:10.1172/jci.insight.139032

**Formigli, L., Benvenuti, S., Mercatelli, R., Quercioli, F., Tani, A., Mirabella, C., Dama, A., Saccardi, R., Mazzanti, B., Cellai, I. et al.** (2012). Dermal matrix scaffold engineered with adult mesenchymal stem cells and platelet-rich plasma as a potential tool for tissue repair and regeneration. *J. Tissue Eng. Regen. Med.* **6**, 125-134. doi:10.1002/term.405

**Foster, K. A., Galeffi, F., Gerich, F. J., Turner, D. A. and Müller, M.** (2006). Optical and pharmacological tools to investigate the role of mitochondria during oxidative stress and neurodegeneration. *Prog. Neurobiol.* **79**, 136-171. doi:10.1016/j.pneurobio.2006.07.001

**Funane, T., Hou, S. S., Zoltowska, K. M., van Veluw, S. J., Berezovska, O., Kumar, A. T. N. and Bacskai, B. J.** (2018). Selective plane illumination microscopy (SPIM) with time-domain fluorescence lifetime imaging microscopy (FLIM) for volumetric measurement of cleared mouse brain samples. *Rev. Sci. Instrum.* **89**, 053705. doi:10.1063/1.5018846

**García-Plazaola, J. I., Fernández-Marín, B., Duke, S. O., Hernández, A., López-Arbeloa, F. and Becerril, J. M.** (2015). Autofluorescence: biological functions and technical applications. *Plant Sci.* **236**, 136-145. doi:10.1016/j.plantsci.2015.03.010

**Ghukasyan, V. V. and Kao, F.-J.** (2009). Monitoring cellular metabolism with fluorescence lifetime of reduced nicotinamide adenine dinucleotide. *J. Phys. Chem. C* **113**, 11532-11540. doi:10.1021/jp810931u

**Ghukasyan, V., Hsu, Y.-Y., Kung, S.-H. and Kao, F.-J.** (2007). Application of fluorescence resonance energy transfer resolved by fluorescence lifetime imaging microscopy for the detection of enterovirus 71 infection in cells. *J. Biomed. Opt.* **12**, 024016. doi:10.1117/1.2718582

**Gioux, S., Mazhar, A. and Cuccia, D. J.** (2019). Spatial frequency domain imaging in 2019: principles, applications, and perspectives. *J. Biomed. Opt.* **24**, 071613. doi:10.1117/1.JBO.24.7.071613

**Glazier, R., Brockman, J. M., Bartle, E., Mattheyses, A. L., Destaing, O. and Salaita, K.** (2019). DNA mechanotechnology reveals that integrin receptors apply pN forces in podosomes on fluid substrates. *Nat. Commun.* **10**, 4507. doi:10.1038/s41467-019-12304-4

**Gómez, C. A., Sutin, J., Wu, W., Fu, B., Uhlirova, H., Devor, A., Boas, D. A., Sakadžić, S. and Yaseen, M. A.** (2018). Phasor analysis of NADH FLIM identifies pharmacological disruptions to mitochondrial metabolic processes in the rodent cerebral cortex. *PLoS ONE* **13**, e0154978. doi:10.1371/journal.pone.0194578

**Greger, K., Neetz, M. J., Reynaud, E. G. and Stelzer, E. H. K.** (2011). Three-dimensional fluorescence lifetime imaging with a single plane illumination microscope provides an improved signal to noise ratio. *Opt. Express* **19**, 20743-20750. doi:10.1364/OE.19.020743

**Greiner, V. J., Shvadchak, V., Fritz, J., Arntz, Y., Didier, P., Frisch, B., Boudier, C., Mély, Y. and DE Rocquigny, H.** (2011). Characterization of the mechanisms of HIV-1 Vpr(52–96) internalization in cells. *Biochimie* **93**, 1647-1658. doi:10.1016/j.biochi.2011.05.033

**Hage, C.-H., Leclerc, P., Fabert, M., Bardet, S. M., Brevier, J., Ducourthial, G., Mansuryan, T., Leray, A., Kudlinski, A. and Louradour, F.** (2019). A readily usable two-photon fluorescence lifetime microendoscope. *J. Biophoton.* **12**, e201800276. doi:10.1002/jbio.201800276

**Hatzenpichler, R., Krukenberg, V., Spietz, R. L. and Jay, Z. J.** (2020). Next-generation physiology approaches to study microbiome function at single cell level. *Nat. Rev. Microbiol.* **18**, 241-256. doi:10.1038/s41579-020-0323-1

**Heaster, T. M., Humayun, M., Yu, J., Beebe, D. J. and Skala, M. C.** (2020). Autofluorescence imaging of 3D tumor-macrophage microscale cultures resolves spatial and temporal dynamics of macrophage metabolism. *Cancer Res.* **80**, 5408-5423. doi:10.1158/0008-5472.can-20-0831

**Hell, S. W. and Wichmann, J.** (1994). Breaking the diffraction resolution limit by stimulated emission: stimulated-emission-depletion fluorescence microscopy. *Opt. Lett.* **19**, 780-782. doi:10.1364/OL.19.000780

**Hirvonen, L. M. and Suhling, K.** (2020). Fast timing techniques in FLIM applications. *Front. Phys.* **8**, 637. doi:10.3389/fphy.2020.00161

**Hirvonen, L. M., Nedbal, J., Almutairi, N., Phillips, T. A., Becker, W., Conneely, T., Milnes, J., Cox, S., Stürzenbaum, S. and Suhling, K.** (2020). Lightsheet fluorescence lifetime imaging microscopy with wide-field time-correlated single photon counting. *J. Biophoton.* **13**, e201960099. doi:10.1002/jbio.201960099

**Holub, O., Seufferheld, M. J., Gohlke, C., Govindjee, and Clegg, R. M.** (2000). Fluorescence Lifetime Imaging (FLI) in real-time - a new technique in photosynthesis research. *Photosynthetica* **38**, 581-599. doi:10.1023/A:1012465508465

**Hoppe, A. D., Shorte, S. L., Swanson, J. A. and Heintzmann, R.** (2008). Three-dimensional FRET reconstruction microscopy for analysis of dynamic molecular interactions in live cells. *Biophys. J.* **95**, 400-418. doi:10.1529/biophysj.107.125385

**Hung, Y. P., Albeck, J. G., Tantama, M. and Yellen, G.** (2011). Imaging cytosolic NADH-NAD+ redox state with a genetically encoded fluorescent biosensor. *Cell Metab.* **14**, 545-554. doi:10.1016/j.cmet.2011.08.012

**Iermak, I., Vink, J., Bader, A. N., Wientjes, E. and van Amerongen, H.** (2016). Visualizing heterogeneity of photosynthetic properties of plant leaves with two-

photon fluorescence lifetime imaging microscopy. *Biochim. Biophys. Acta Bioener.* **1857**, 1473-1478. doi:10.1016/j.bbabio.2016.05.005
**Ishikawa-Ankerhold, H. C., Ankerhold, R. and Drummen, G. P. C.** (2012). Advanced fluorescence microscopy techniques—Frap, Flip, Flap, Fret and flim. *Molecules* **17**, 4047-4132. doi:10.3390/molecules17044047
**Jenkins, J., Dmitriev, R. I., Morten, K., Mcdermott, K. W. and Papkovsky, D. B.** (2015). Oxygen-sensing scaffolds for 3-dimensional cell and tissue culture. *Acta Biomater.* **16**, 126-135. doi:10.1016/j.actbio.2015.01.032
**Jenkins, J., Borisov, S. M., Papkovsky, D. B. and Dmitriev, R. I.** (2016). Sulforhodamine nanothermometer for multi-parametric fluorescence lifetime imaging microscopy. *Anal. Chem.* **88**, 10566-10572. doi:10.1021/acs.analchem.6b02675
**Jo, J. A., Cheng, S., Cuenca-Martinez, R., Duran-Sierra, E., Malik, B., Ahmed, B., Maitland, K., Cheng, Y.-S. L., Wright, J. and Reese, T.** (2018). Endogenous Fluorescence Lifetime Imaging (FLIM) endoscopy for early detection of oral cancer and dysplasia. In *40th Annual International Conference of the IEEE Engineering in Medicine and Biology Society (EMBC)*, pp. 3009-3012. IEEE. doi:10.1109/EMBC.2018.8513027
**Jones, D. M. and Padilla-Parra, S.** (2015). Imaging real-time HIV-1 virion fusion with FRET-based biosensors. *Sci. Rep.* **5**, 13449. doi:10.1038/srep13449
**Kalinina, S., Breymayer, J., Schäfer, P., Calzia, E., Shcheslavskiy, V., Becker, W. and Rück, A.** (2016). Correlative NAD(P)H-FLIM and oxygen sensing-PLIM for metabolic mapping. *J. Biophoton.* **9**, 800-811. doi:10.1002/jbio.201500297
**Kantelhardt, S. R., Kalasauskas, D., König, K., Kim, E., Weinigel, M., Uchugonova, A. and Giese, A.** (2016). In vivo multiphoton tomography and fluorescence lifetime imaging of human brain tumor tissue. *J. Neurooncol.* **127**, 473-482. doi:10.1007/s11060-016-2062-8
**Kawanabe, S., Araki, Y., Uchimura, T. and Imasaka, T.** (2015). Applying fluorescence lifetime imaging microscopy to evaluate the efficacy of anticancer drugs. *Method Appl. Fluorescence* **3**, 025006. doi:10.1088/2050-6120/3/2/025006
**Kawashima, M., Bensaad, K., Zois, C. E., Barberis, A., Bridges, E., Wigfield, S., Lagerholm, C., Dmitriev, R. I., Tokiwa, M., Toi, M. et al.** (2020). Disruption of hypoxia-inducible fatty acid binding protein 7 induces beige fat-like differentiation and thermogenesis in breast cancer cells. *Cancer Metab.* **8**, 13. doi:10.1186/s40170-020-00219-4
**Kingsley, D. M., Roberge, C. L., Rudkouskaya, A., Faulkner, D. E., Barroso, M., Intes, X. and Corr, D. T.** (2019). Laser-based 3D bioprinting for spatial and size control of tumor spheroids and embryoid bodies. *Acta Biomater.* **95**, 357-370. doi:10.1016/j.actbio.2019.02.014
**König, K.** (2020). Clinical in vivo multiphoton FLIM tomography. *Methods Appl. Fluorescence* **8**, 034002. doi:10.1088/2050-6120/ab8808
**Kuchibhotla, K. V., Lattarulo, C. R., Hyman, B. T. and Bacskai, B. J.** (2009). Synchronous hyperactivity and intercellular calcium waves in astrocytes in Alzheimer mice. *Science* **323**, 1211-1215. doi:10.1126/science.1169096
**Kühl, M., Rickelt, L. F. and Thar, R.** (2007). Combined imaging of bacteria and oxygen in biofilms. *Appl. Environ. Microbiol.* **73**, 6289-6295. doi:10.1128/AEM.01574-07
**Kuimova, M. K.** (2012). Mapping viscosity in cells using molecular rotors. *Phys. Chem. Chem. Phys.* **14**, 12671-12686. doi:10.1039/c2cp41674c
**Kumar, A. T. N., Hou, S. S. and Rice, W. L.** (2018). Tomographic fluorescence lifetime multiplexing in the spatial frequency domain. *Optica* **5**, 624-627. doi:10.1364/OPTICA.5.000624
**Lakowicz, J. R., Szmacinski, H., Nowaczyk, K. and Johnson, M. L.** (1992). Fluorescence lifetime imaging of free and protein-bound NADH. *Proc. Natl Acad. Sci. USA* **89**, 1271-1275. doi:10.1073/pnas.89.4.1271
**Lattarulo, C., Thyssen, D., Kuchibholta, K. V., Hyman, B. T. and Bacskaiq, B. J.** (2011). Microscopic imaging of intracellular calcium in live cells using lifetime-based ratiometric measurements of Oregon Green BAPTA-1. *Neurodegeneration* **793**, 377-389. doi:10.1007/978-1-61779-328-8_25
**Laurent, J., Blin, G., Chatelain, F., Vanneaux, V., Fuchs, A., Larghero, J. and Théry, M.** (2017). Convergence of microengineering and cellular self-organization towards functional tissue manufacturing. *Nat. Biomed. Eng.* **1**, 939-956. doi:10.1038/s41551-017-0166-x
**Le Marois, A. and Suhling, K.** (2017). Quantitative live cell FLIM imaging in three dimensions. *Adv. Exp. Med. Biol.* **1035**, 31-48. doi:10.1007/978-3-319-67358-5_3
**Leben, R., Köhler, M., Radbruch, H., Hauser, A. E. and Niesner, R. A.** (2019). Systematic enzyme mapping of cellular metabolism by phasor-analyzed label-free NAD(P)H fluorescence lifetime imaging. *Int. J. Mol. Sci.* **20**, 5565. doi:10.3390/ijms20225565
**Leblond, F., Davis, S. C., Valdés, P. A. and Pogue, B. W.** (2010). Pre-clinical whole-body fluorescence imaging: review of instruments, methods and applications. *J. Photochem. Photobiol. B Biol.* **98**, 77-94. doi:10.1016/j.jphotobiol.2009.11.007
**Lee, M. W., Song, J. W., Kang, W. J., Nam, H. S., Kim, T. S., Kim, S., Oh, W.-Y., Kim, J. W. and Yoo, H.** (2018). Comprehensive intravascular imaging of atherosclerotic plaque in vivo using optical coherence tomography and fluorescence lifetime imaging. *Sci. Rep.* **8**, 14561. doi:10.1038/s41598-018-32951-9
**Lei, R., Jiang, H., Hu, F., Yan, J. and Zhu, S.** (2017). Chlorophyll fluorescence lifetime imaging provides new insight into the chlorosis induced by plant virus infection. *Plant Cell Rep.* **36**, 327-341. doi:10.1007/s00299-016-2083-y
**Levitt, J. A., Matthews, D. R., Ameer-Beg, S. M. and Suhling, K.** (2009). Fluorescence lifetime and polarization-resolved imaging in cell biology. *Curr. Opin. Biotechnol.* **20**, 28-36. doi:10.1016/j.copbio.2009.01.004
**Levitt, J. A., Chung, P.-H. and Suhling, K.** (2015). Spectrally resolved fluorescence lifetime imaging of Nile red for measurements of intracellular polarity. *J. Biomed. Opt.* **20**, 096002. doi:10.1117/1.JBO.20.9.096002
**Li, R., Liu, A., Wu, T., Xiao, W., Tang, L. and Chen, L.** (2020). Digital scanned laser light-sheet fluorescence lifetime microscopy with wide-field time-gated imaging. *J. Microsc.* **279**, 69-76. doi:10.1111/jmi.12898
**Libanje, F., Raingeaud, J., Luan, R., Thomas, Z. A., Zajac, O., Veiga, J., Marisa, L., Adam, J., Boige, V., Malka, D. et al.** (2019). ROCK 2 inhibition triggers the collective invasion of colorectal adenocarcinomas. *EMBO J.* **38**, e99299. doi:10.15252/embj.201899299
**Liu, T.-L., Upadhyayula, S., Milkie, D. E., Singh, V., Wang, K., Swinburne, I. A., Mosaliganti, K. R., Collins, Z. M., Hiscock, T. W., Shea, J. et al.** (2018a). Observing the cell in its native state: imaging subcellular dynamics in multicellular organisms. *Science* **360**, eaaq1392. doi:10.1126/science.aaq1392
**Liu, Z., Pouli, D., Alonzo, C. A., Varone, A., Karaliota, S., Quinn, K. P., Münger, K., Karalis, K. P. and Georgakoudi, I.** (2018b). Mapping metabolic changes by noninvasive, multiparametric, high-resolution imaging using endogenous contrast. *Sci. Adv.* **4**, eaap9302. doi:10.1126/sciadv.aap9302
**Llères, D., Bailly, A. P., Perrin, A., Norman, D. G., Xirodimas, D. P. and Feil, R.** (2017). Quantitative FLIM-FRET microscopy to monitor nanoscale chromatin compaction in vivo reveals structural roles of condensin complexes. *Cell Rep.* **18**, 1791-1803. doi:10.1016/j.celrep.2017.01.043
**Looger, L. L. and Griesbeck, O.** (2012). Genetically encoded neural activity indicators. *Curr. Opin. Neurobiol.* **22**, 18-23. doi:10.1016/j.conb.2011.10.024
**Lou, J., Scipioni, L., Wright, B. K., Bartolec, T. K., Zhang, J., Masamsetti, V. P., Gaus, K., Gratton, E., Cesare, A. J. and Hinde, E.** (2019). Phasor histone FLIM-FRET microscopy quantifies spatiotemporal rearrangement of chromatin architecture during the DNA damage response. *Proc. Natl Acad. Sci. USA* **116**, 7323-7332. doi:10.1073/pnas.1814965116
**Lu, S., Ouyang, M., Seong, J., Zhang, J., Chien, S. and Wang, Y.** (2008). The spatiotemporal pattern of Src activation at lipid rafts revealed by diffusion-corrected FRET imaging. *PLoS Comput. Biol.* **4**, e1000127. doi:10.1371/journal.pcbi.1000127
**Lu, M., Williamson, N., Mishra, A., Michel, C. H., Kaminski, C. F., Tunnacliffe, A. and Kaminski Schierle, G. S.** (2019). Structural progression of amyloid-β Arctic mutant aggregation in cells revealed by multiparametric imaging. *J. Biol. Chem.* **294**, 1478-1487. doi:10.1074/jbc.RA118.004511
**Ma, Y., Benda, A., Kwiatek, J., Owen, D. M. and Gaus, K.** (2018). Time-resolved Laurdan fluorescence reveals insights into membrane viscosity and hydration levels. *Biophys. J.* **115**, 1498-1508. doi:10.1016/j.bpj.2018.08.041
**Ma, N., de Mochel, N. R., Pham, P. D., Yoo, T. Y., Cho, K. W. and Digman, M. A.** (2019). Label-free assessment of pre-implantation embryo quality by the Fluorescence Lifetime Imaging Microscopy (FLIM)-phasor approach. *Sci. Rep.* **9**, 13206. doi:10.1038/s41598-019-48107-2
**Malacrida, L. and Gratton, E.** (2018). LAURDAN fluorescence and phasor plots reveal the effects of a H2O2 bolus in NIH-3T3 fibroblast membranes dynamics and hydration. *Free Radic. Biol. Med.* **128**, 144-156. doi:10.1016/j.freeradbiomed.2018.06.004
**Mannam, V., Zhang, Y., Yuan, X., Ravasio, C. and Howard, S. S.** (2020). Machine learning for faster and smarter fluorescence lifetime imaging microscopy. *J. Phys. Photonics* **2**, 042005. doi:10.1088/2515-7647/abac1a
**Martin-Fernandez, M., Longshaw, S. V., Kirby, I., Santis, G., Tobin, M. J., Clarke, D. T. and Jones, G. R.** (2004). Adenovirus type-5 entry and disassembly followed in living cells by Fret, fluorescence anisotropy, and FLIM. *Biophys. J.* **87**, 1316-1327. doi:10.1529/biophysj.103.035444
**Masters, B. R., So, P. T. and Gratton, E.** (1998). Multiphoton excitation microscopy of in vivo human skin: functional and morphological optical biopsy based on three-dimensional imaging, lifetime measurements and fluorescence spectroscopy. *Ann. N. Y. Acad. Sci.* **838**, 58-67. doi:10.1111/j.1749-6632.1998.tb08187.x
**Masullo, L. A., Steiner, F., Zähringer, J., Lopez, L. F., Bohlen, J., Richter, L., Cole, F., Tinnefeld, P. and Stefani, F. D.** (2020). Pulsed Interleaved MINFLUX. *Nano Lett.* **21**, 840-846. doi:10.1021/acs.nanolett.0c04600
**McConnell, G. and Amos, W. B.** (2018). Application of the Mesolens for subcellular resolution imaging of intact larval and whole adult Drosophila. *J. Microsc.* **270**, 252-258. doi:10.1111/jmi.12693
**McConnell, G., Trägårdh, J., Amor, R., Dempster, J., Reid, E. and Amos, W. B.** (2016). A novel optical microscope for imaging large embryos and tissue volumes with sub-cellular resolution throughout. *eLife* **5**, e18659. doi:10.7554/eLife.18659
**McGhee, E. J., Morton, J. P., von Kriegsheim, A., Schwarz, J. P., Karim, S. A., Carragher, N. O., Sansom, O. J., Anderson, K. I. and Timpson, P.** (2011). FLIM-FRET imaging in vivo reveals 3D-environment spatially regulates RhoGTPase activity during cancer cell invasion. *Small GTPases* **2**, 239-244. doi:10.4161/sgtp.2.4.17275

**McGinty, J., Taylor, H. B., Chen, L., Bugeon, L., Lamb, J. R., Dallman, M. J. and French, P. M. W.** (2011). In vivo fluorescence lifetime optical projection tomography. *Biomed. Opt. Express* **2**, 1340-1350. doi:10.1364/BOE.2.001340

**Mehidine, H., Chalumeau, A., Poulon, F., Jamme, F., Varlet, P., Devaux, B., Refregiers, M. and ABI Haidar, D.** (2019). Optical signatures derived from deep UV to NIR excitation discriminates healthy samples from low and high grades glioma. *Sci. Rep.* **9**, 8786. doi:10.1038/s41598-019-45181-4

**Meleshina, A. V., Rogovaya, O. S., Dudenkova, V. V., Sirotkina, M. A., Lukina, M. M., Bystrova, A. S., Krut, V. G., Kuznetsova, D. S., Kalabusheva, E. P., Vasiliev, A. V. et al.** (2018). Multimodal label-free imaging of living dermal equivalents including dermal papilla cells. *Stem Cell Res. Ther.* **9**, 84. doi:10.1186/s13287-018-0838-9

**Meyer-Almes, F.-J.** (2017). Fluorescence lifetime based bioassays. *Methods Appl. Fluorescence* **5**, 042002. doi:10.1088/2050-6120/aa7c7a

**Mik, E. G., Stap, J., Sinaasappel, M., Beek, J. F., Aten, J. A., van Leeuwen, T. G. and Ince, C.** (2006). Mitochondrial $PO_2$ measured by delayed fluorescence of endogenous protoporphyrin IX. *Nat. Methods* **3**, 939-945. doi:10.1038/nmeth940

**Mitchell, C. A., Poland, S. P., Seyforth, J., Nedbal, J., Gelot, T., Huq, T., Holst, G., Knight, R. D. and Ameer-Beg, S. M.** (2017). Functional in vivo imaging using fluorescence lifetime light-sheet microscopy. *Opt. Lett.* **42**, 1269-1272. doi:10.1364/OL.42.001269

**Mizukami, K., Katano, A., Shiozaki, S., Yoshihara, T., Goda, N. and Tobita, S.** (2020). In vivo O2 imaging in hepatic tissues by phosphorescence lifetime imaging microscopy using Ir(III) complexes as intracellular probes. *Sci. Rep.* **10**, 1-14. doi:10.1038/s41598-020-76878-6

**Mizuno, T., Hase, E., Minamikawa, T., Tokizane, Y., Oe, R., Koresawa, H., Yamamoto, H. and Yasui, T.** (2021). Full-field fluorescence lifetime dual-comb microscopy using spectral mapping and frequency multiplexing of dual-comb optical beats. *Sci. Adv.* **7**, eabd2102. doi:10.1126/sciadv.abd2102

**Mohammed, Y. H., Barkauskas, D. S., Holmes, A., Grice, J. and Roberts, M. S.** (2020). Noninvasive in vivo human multiphoton microscopy: a key method in proving nanoparticulate zinc oxide sunscreen safety. *J. Biomed. Opt.* **25**, 014509. doi:10.1117/1.JBO.25.1.014509

**Mongeon, R., Venkatachalam, V. and Yellen, G.** (2016). Cytosolic NADH-NAD(+) redox visualized in brain slices by two-photon fluorescence lifetime biosensor imaging. *Antioxid Redox Signal.* **25**, 553-563. doi:10.1089/ars.2015.6593

**Moßhammer, M., Brodersen, K. E., Kühl, M. and Koren, K.** (2019). Nanoparticle- and microparticle-based luminescence imaging of chemical species and temperature in aquatic systems: a review. *Microchimica Acta* **186**, 126. doi:10.1007/s00604-018-3202-y

**Nam, H. S., Kang, W. J., Lee, M. W., Song, J. W., Kim, J. W., Oh, W.-Y. and Yoo, H.** (2018). Multispectral analog-mean-delay fluorescence lifetime imaging combined with optical coherence tomography. *Biomed. Opt. Express* **9**, 1930-1947. doi:10.1364/BOE.9.001930

**Napp, J., Behnke, T., Fischer, L., WüRth, C., Wottawa, M., Katschinski, D. R. M., Alves, F., Resch-Genger, U. and Schäferling, M.** (2011). Targeted luminescent near-infrared polymer-nanoprobes for in vivo imaging of tumor hypoxia. *Anal. Chem.* **83**, 9039-9046. doi:10.1021/ac201870b

**Neto, N., Dmitriev, R. I. and Monaghan, M. G.** (2020). Seeing is believing: noninvasive microscopic imaging modalities for tissue engineering and regenerative medicine. In *Cell Engineering and Regeneration* (ed. J. M. Gimble, D. Marolt Presen, R. Oreffo, H. Redl and S. Wolbank), pp. 1-41. Cham: Springer International Publishing.

**Neu, T. R., Walczysko, P. and Lawrence, J. R.** (2004). Two-photon imaging for studying the microbial ecology of biofilm systems. *Microbes Environ.* **19**, 1-6. doi:10.1264/jsme2.19.1

**Nia, H. T., Munn, L. L. and Jain, R. K.** (2020). Physical traits of cancer. *Science* **370**, eaaz0868. doi:10.1126/science.aaz0868

**Niehörster, T., Löschberger, A., Gregor, I., Krämer, B., Rahn, H.-J., Patting, M., Koberling, F., Enderlein, J. and Sauer, M.** (2016). Multi-target spectrally resolved fluorescence lifetime imaging microscopy. *Nat. Methods* **13**, 257-262. doi:10.1038/nmeth.3740

**Nobis, M., Carragher, N. O., Mcghee, E. J., Morton, J. P., Sansom, O. J., Anderson, K. I. and Timpson, P.** (2013). Advanced intravital subcellular imaging reveals vital three-dimensional signalling events driving cancer cell behaviour and drug responses in live tissue. *FEBS J.* **280**, 5177-5197. doi:10.1111/febs.12348

**Nothdurft, R. E., Patwardhan, S. V., Akers, W. J., Ye, Y., Achilefu, S. and Culver, J. P.** (2009). In vivo fluorescence lifetime tomography. *J. Biomed. Opt.* **14**, 024004. doi:10.1117/1.3086607

**Ntziachristos, V.** (2010). Going deeper than microscopy: the optical imaging frontier in biology. *Nat. Methods* **7**, 603-614. doi:10.1038/nmeth.1483

**Ochoa, M., Rudkouskaya, A., Yao, R., Yan, P., Barroso, M. and Intes, X.** (2020). High compression deep learning based single-pixel hyperspectral macroscopic fluorescence lifetime imaging in vivo. *Biomed. Opt. Exp.* **11**, 5401-5424. doi:10.1364/BOE.396771

**O'donnell, N., Okkelman, I. A., Timashev, P., Gromovykh, T. I., Papkovsky, D. B. and Dmitriev, R. I.** (2018). Cellulose-based scaffolds for fluorescence lifetime imaging-assisted tissue engineering. *Acta Biomater.* **80**, 85-96. doi:10.1016/j.actbio.2018.09.034

**Ogle, M. M., Smith McWilliams, A. D., Jiang, B. and Martí, A. A.** (2020). Latest trends in temperature sensing by molecular probes. *ChemPhotoChem* **4**, 255-270. doi:10.1002/cptc.201900255

**Okkelman, I. A., Dmitriev, R. I., Foley, T. and Papkovsky, D. B.** (2016). Use of Fluorescence Lifetime Imaging Microscopy (FLIM) as a timer of cell cycle S phase. *PLoS ONE* **11**, e0167385. doi:10.1371/journal.pone.0167385

**Okkelman, I. A., Foley, T., Papkovsky, D. B. and Dmitriev, R. I.** (2017a). Live cell imaging of mouse intestinal organoids reveals heterogeneity in their oxygenation. *Biomaterials* **146**, 86-96. doi:10.1016/j.biomaterials.2017.08.043

**Okkelman, I. A., Foley, T., Papkovsky, D. B. and Dmitriev, R. I.** (2017b). Multi-parametric imaging of hypoxia and cell cycle in intestinal organoid culture. *Multi-Parametric Live Cell Microsc. 3D Tissue Models* **1035**, 85-103. doi:10.1007/978-3-319-67358-5_6

**Okkelman, I. A., Papkovsky, D. B. and Dmitriev, R. I.** (2019). Estimation of the mitochondrial membrane potential using fluorescence lifetime imaging microscopy. *Cytometry Part A* **97**, 471-482. doi:10.1002/cyto.a.23886

**Okkelman, I. A., Mcgarrigle, R., O'carroll, S., Berrio, D. C., Schenke-Layland, K., Hynes, J. and Dmitriev, R. I.** (2020a). Extracellular Ca2+-sensing fluorescent protein biosensor based on a collagen-binding domain. *ACS Appl. Bio Materials* **3**, 5310-5321. doi:10.1021/acsabm.0c00649

**Okkelman, I. A., Neto, N., Papkovsky, D. B., Monaghan, M. G. and Dmitriev, R. I.** (2020b). A deeper understanding of intestinal organoid metabolism revealed by combining fluorescence lifetime imaging microscopy (FLIM) and extracellular flux analyses. *Redox Biol.* **30**, 101420. doi:10.1016/j.redox.2019.101420

**Okkelman, I. A., Puschhof, J., Papkovsky, D. B. and Dmitriev, R. I.** (2020c). Visualization of stem cell niche by fluorescence lifetime imaging microscopy. In *Intestinal Stem Cells: Methods and Protocols* (ed. P. Ordóñez-Morán), pp. 65-97. New York, NY: Springer US.

**Ovečka, M., von Wangenheim, D., Tomančák, P., Šamajová, O., Komis, G. and Šamaj, J.** (2018). Multiscale imaging of plant development by light-sheet fluorescence microscopy. *Nat. plants* **4**, 639-650. doi:10.1038/s41477-018-0238-2

**Owen, D. M., Neil, M. A. A., French, P. M. W. and Magee, A. I.** (2007). Optical techniques for imaging membrane lipid microdomains in living cells. *Semin. Cell Dev. Biol.* **18**, 591-598. doi:10.1016/j.semcdb.2007.07.011

**Oxborough, K. and Baker, N. R.** (1997). An instrument capable of imaging chlorophyll a fluorescence from intact leaves at very low irradiance and at cellular and subcellular levels of organization. *Plant Cell Environ.* **20**, 1473-1483. doi:10.1046/j.1365-3040.1997.d01-42.x

**Ozturk, M. S., Chen, C.-W., Ji, R., Zhao, L., Nguyen, B.-N. B., Fisher, J. P., Chen, Y. and Intes, X.** (2016). Mesoscopic fluorescence molecular tomography for evaluating engineered tissues. *Ann. Biomed. Eng.* **44**, 667-679. doi:10.1007/s10439-015-1511-4

**Ozturk, M. S., Lee, V. K., Zou, H., Friedel, R. H., Intes, X. and Dai, G.** (2020). High-resolution tomographic analysis of in vitro 3D glioblastoma tumor model under long-term drug treatment. *Sci. Adv.* **6**, eaay7513. doi:10.1126/sciadv.aay7513

**Page, H., Flood, P. and Reynaud, E. G.** (2013). Three-dimensional tissue cultures: current trends and beyond. *Cell Tissue Res.* **352**, 123-131. doi:10.1007/s00441-012-1441-5

**Pal, R., Kang, H., Choi, H. S. and Kumar, A. T. N.** (2019). Fluorescence lifetime-based tumor contrast enhancement using an EGFR antibody–labeled near-infrared fluorophore. *Clin. Cancer Res.* **25**, 6653-6661. doi:10.1158/1078-0432.CCR-19-1686

**Pampaloni, F., Reynaud, E. G. and Stelzer, E. H. K.** (2007). The third dimension bridges the gap between cell culture and live tissue. *Nat. Rev. Mol. Cell Biol.* **8**, 839-845. doi:10.1038/nrm2236

**Pande, P., Shrestha, S., Park, J., Gimenez-Conti, I., Brandon, J., Applegate, B. E. and Jo, J. A.** (2016). Automated analysis of multimodal fluorescence lifetime imaging and optical coherence tomography data for the diagnosis of oral cancer in the hamster cheek pouch model. *Biomed. Opt. Exp.* **7**, 2000-2015. doi:10.1364/BOE.7.002000

**Papkovsky, D. B. and Dmitriev, R. I.** (2013). Biological detection by optical oxygen sensing. *Chem. Soc. Rev.* **42**, 8700-8732. doi:10.1039/c3cs60131e

**Papkovsky, D. and Dmitriev, R.** (2018a). *Quenched-phosphorescence Detection of Molecular Oxygen: Applications in Life Sciences*. The Royal Society of Chemistry.

**Papkovsky, D. B. and Dmitriev, R. I.** (2018b). Imaging of oxygen and hypoxia in cell and tissue samples. *Cell. Mol. Life Sci.* **75**, 2963-2980. doi:10.1007/s00018-018-2840-x

**Papour, A., Taylor, Z. D., Sherman, A. J., Sanchez, D., Lucey, G., Liau, L., Stafsudd, O. M., Yong, W. H. and Grundfest, W. S.** (2013). Optical imaging for brain tissue characterization using relative fluorescence lifetime imaging. *J. Biomed. Opt.* **18**, 060504. doi:10.1117/1.JBO.18.6.060504

**Periasamy, A.** (2001). *Methods in Cellular Imaging*. Springer.

**Perottoni, S., Neto, N. G. B., Di Nitto, C., Dmitriev, R. I., Raimondi, M. T. and Monaghan, M. G.** (2021). Intracellular label-free detection of mesenchymal stem cell metabolism within a perivascular niche-on-a-chip. *Lab Chip* **21**, 1395-1408. doi:10.1039/D0LC01034K

**Petrášek, Z., Eckert, H.-J. and Kemnitz, K.** (2009). Wide-field photon counting fluorescence lifetime imaging microscopy: application to photosynthesizing systems. *Photosynth. Res.* **102**, 157. doi:10.1007/s11120-009-9444-0

**Pian, Q., Yao, R., Sinsuebphon, N. and Intes, X.** (2017). Compressive hyperspectral time-resolved wide-field fluorescence lifetime imaging. *Nat. Photonics* **11**, 411. doi:10.1038/nphoton.2017.82

**Piston, D. W. and Kremers, G.-J.** (2007). Fluorescent protein FRET: the good, the bad and the ugly. *Trends Biochem. Sci.* **32**, 407-414. doi:10.1016/j.tibs.2007.08.003

**Poëa-Guyon, S., Pasquier, H., Mérola, F., Morel, N. and Erard, M.** (2013). The enhanced cyan fluorescent protein: a sensitive pH sensor for fluorescence lifetime imaging. *Anal. Bioanal. Chem.* **405**, 3983-3987. doi:10.1007/s00216-013-6860-y

**Poudel, C., Mela, I. and Kaminski, C. F.** (2020). High-throughput, multi-parametric, and correlative fluorescence lifetime imaging. *Methods Appl. Fluorescence* **8**, 024005. doi:10.1088/2050-6120/ab7364

**Quaranta, M., Borisov, S. M. and Klimant, I.** (2012). Indicators for optical oxygen sensors. *Bioanal. Rev.* **4**, 115-157. doi:10.1007/s12566-012-0032-y

**Radbruch, H., Bremer, D., Mothes, R., Günther, R., Rinnenthal, J. L., Pohlan, J., Ulbricht, C., Hauser, A. E. and Niesner, R.** (2015). Intravital FRET: probing cellular and tissue function in vivo. *Int. J. Mol. Sci.* **16**, 11713-11727. doi:10.3390/ijms160511713

**Rajoria, S., Zhao, L., Intes, X. and Barroso, M.** (2014). FLIM-FRET for cancer applications. *Curr. Mol. Imaging* **3**, 144-161. doi:10.2174/2211555203666141117221111

**Rakymzhan, A., Radbruch, H. and Niesner, R. A.** (2017). Quantitative imaging of $Ca^{2+}$ by 3D–FLIM in live tissues. *Multi-Parametric Live Cell Microsc. 3D Tissue Models* **1035**, 135-141. doi:10.1007/978-3-319-67358-5_9

**Ranawat, H., Pal, S. and Mazumder, N.** (2019). Recent trends in two-photon auto-fluorescence lifetime imaging (2P-FLIM) and its biomedical applications. *Biomed. Eng. Lett.* **9**, 293-310. doi:10.1007/s13534-019-00119-7

**Raspe, M., Kedziora, K. M., van den Broek, B., Zhao, Q., DE Jong, S., Herz, J., Mastop, M., Goedhart, J., Gadella, T. W. J., Young, I. T.** and et al. (2016). siFLIM: single-image frequency-domain FLIM provides fast and photon-efficient lifetime data. *Nat. Methods* **13**, 501-504. doi:10.1038/nmeth.3836

**Rice, W. L., Shcherbakova, D. M., Verkhusha, V. V. and Kumar, A. T. N.** (2015). In vivo tomographic imaging of deep-seated cancer using fluorescence lifetime contrast. *Cancer Res.* **75**, 1236-1243. doi:10.1158/0008-5472.CAN-14-3001

**Rich, R. M., Stankowska, D. L., Maliwal, B. P., Sørensen, T. J., Laursen, B. W., Krishnamoorthy, R. R., Gryczynski, Z., Borejdo, J., Gryczynski, I. and Fudala, R.** (2013). Elimination of autofluorescence background from fluorescence tissue images by use of time-gated detection and the AzaDiOxaTriAngulenium (ADOTA) fluorophore. *Anal. Bioanal. Chem.* **405**, 2065-2075. doi:10.1007/s00216-012-6623-1

**Rico-Jimenez, J., Lee, J. H., Alex, A., Musaad, S., Chaney, E., Barkalifa, R., Olson, E., Adams, D., Marjanovic, M., Arp, Z. et al.** (2020). Non-invasive monitoring of pharmacodynamics during the skin wound healing process using multimodal optical microscopy. *BMJ Open Diabetes Res. Care* **8**, e000974. doi:10.1136/bmjdrc-2019-000974

**Ringer, P., Weiss, A., Cost, A.-L., Freikamp, A., Sabass, B., Mehlich, A., Tramier, M., Rief, M. and Grashoff, C.** (2017). Multiplexing molecular tension sensors reveals piconewton force gradient across talin-1. *Nat. Methods* **14**, 1090-1096. doi:10.1038/nmeth.4431

**Rinnenthal, J. L., Börnchen, C., Radbruch, H., Andresen, V., Mossakowski, A., Siffrin, V., Seelemann, T., Spiecker, H., Moll, I., Herz, J. et al.** (2013). Parallelized TCSPC for dynamic intravital fluorescence lifetime imaging: quantifying neuronal dysfunction in neuroinflammation. *PLoS ONE* **8**, e60100. doi:10.1371/journal.pone.0060100

**Rino, J. and Carmo-Fonseca, M.** (2009). The spliceosome: a self-organized macromolecular machine in the nucleus? *Trends Cell Biol.* **19**, 375-384. doi:10.1016/j.tcb.2009.05.004

**Rios, A. C. and Clevers, H.** (2018). Imaging organoids: a bright future ahead. *Nat. Methods* **15**, 24. doi:10.1038/nmeth.4537

**Rodríguez-Colman, M. J., Schewe, M., Meerlo, M., Stigter, E., Gerrits, J., Pras-Raves, M., Sacchetti, A., Hornsveld, M., Oost, K. C., Snippert, H. J. et al.** (2017). Interplay between metabolic identities in the intestinal crypt supports stem cell function. *Nature* **543**, 424-427. doi:10.1038/nature21673

**Roussakis, E., Li, Z., Nichols, A. J. and Evans, C. L.** (2015). Oxygen-sensing methods in biomedicine from the macroscale to the microscale. *Angewandte Chem. Int. Edn.* **54**, 8340-8362. doi:10.1002/anie.201410646

**Rudkouskaya, A., Sinsuebphon, N., Ward, J., Tubbesing, K., Intes, X. and Barroso, M.** (2018). Quantitative imaging of receptor-ligand engagement in intact live animals. *J. Control. Release* **286**, 451-459. doi:10.1016/j.jconrel.2018.07.032

**Rudkouskaya, A., Sinsuebphon, N., Ochoa, M., Chen, S.-J., Mazurkiewicz, J. E., Intes, X. and Barroso, M.** (2020a). Multiplexed non-invasive tumor imaging of glucose metabolism and receptor-ligand engagement using dark quencher FRET acceptor. *Theranostics* **10**, 10309-10325. doi:10.7150/thno.45825

**Rudkouskaya, A., Smith, J. T., Intes, X. and Barroso, M.** (2020b). Quantification of Trastuzumab–HER2 engagement in vitro and in vivo. *Molecules* **25**, 5976. doi:10.3390/molecules25245976

**Rytelewski, M., Haryutyunan, K., Nwajei, F., Shanmugasundaram, M., Wspanialy, P., Zal, M. A., Chen, C.-H., El Khatib, M., Plunkett, S., Vinogradov, S. A. et al.** (2019). Merger of dynamic two-photon and phosphorescence lifetime microscopy reveals dependence of lymphocyte motility on oxygen in solid and hematological tumors. *J. Immunother. Cancer* **7**, 78. doi:10.1186/s40425-019-0543-y

**Sakadžić, S., Roussakis, E., Yaseen, M. A., Mandeville, E. T., Srinivasan, V. J., Arai, K., Ruvinskaya, S., Devor, A., Lo, E. H., Vinogradov, S. A. et al.** (2010). Two-photon high-resolution measurement of partial pressure of oxygen in cerebral vasculature and tissue. *Nat. Methods* **7**, 755-759. doi:10.1038/nmeth.1490

**Sarder, P., Maji, D. and Achilefu, S.** (2015). Molecular probes for fluorescence lifetime imaging. *Bioconjug. Chem.* **26**, 963-974. doi:10.1021/acs.bioconjchem.5b00167

**Schilling, K., El Khatib, M., Plunkett, S., Xue, J., Xia, Y., Vinogradov, S. A., Brown, E. and Zhang, X.** (2019). Electrospun fiber mesh for high-resolution measurements of oxygen tension in cranial bone defect repair. *ACS Appl. Mater. Interfaces* **11**, 33548-33558. doi:10.1021/acsami.9b08341

**Schlafer, S. and Meyer, R. L.** (2017). Confocal microscopy imaging of the biofilm matrix. *J. Microbiol. Methods* **138**, 50-59. doi:10.1016/j.mimet.2016.03.002

**Schreiber, G., Barberis, M., Scolari, S., Klaus, C., Herrmann, A. and Klipp, E.** (2012). Unraveling interactions of cell cycle-regulating proteins Sic1 and B-type cyclins in living yeast cells: a FLIM-FRET approach. *FASEB J.* **26**, 546-554. doi:10.1096/fj.11-192518

**Seidenari, S., Arginelli, F., Dunsby, C., French, P. M., König, K., Magnoni, C., Talbot, C. and Ponti, G.** (2013). Multiphoton laser tomography and fluorescence lifetime imaging of melanoma: morphologic features and quantitative data for sensitive and specific non-invasive diagnostics. *PLoS ONE* **8**, e70682. doi:10.1371/journal.pone.0070682

**Shapiro, O. H., Kramarsky-Winter, E., Gavish, A. R., Stocker, R. and Vardi, A.** (2016). A coral-on-a-chip microfluidic platform enabling live-imaging microscopy of reef-building corals. *Nat. Commun.* **7**, 10860. doi:10.1038/ncomms10860

**Sharpe, J., Ahlgren, U., Perry, P., Hill, B., Ross, A., Hecksher-Sørensen, J., Baldock, R. and Davidson, D.** (2002). Optical projection tomography as a tool for 3D microscopy and gene expression studies. *Science* **296**, 541-545. doi:10.1126/science.1068206

**Shcheslavskiy, V. I., Shirmanova, M. V., Dudenkova, V. V., Lukyanov, K. A., Gavrina, A. I., Shumilova, A. V., Zagaynova, E. and Becker, W.** (2018). Fluorescence time-resolved macroimaging. *Opt. Lett.* **43**, 3152-3155. doi:10.1364/OL.43.003152

**Sherlock, B. E., Phipps, J. E., Bec, J. and Marcu, L.** (2017). Simultaneous, label-free, multispectral fluorescence lifetime imaging and optical coherence tomography using a double-clad fiber. *Opt. Lett.* **42**, 3753-3756. doi:10.1364/OL.42.003753

**Sherrard, A., Bishop, P., Panagi, M., Villagomez, M. B., Alibhai, D. and Kaidi, A.** (2018). Streamlined histone-based fluorescence lifetime imaging microscopy (FLIM) for studying chromatin organisation. *Biol. Open* **7**, bio031476. doi:10.1242/bio.031476

**Shirmanova, M. V., Shimolina, L. E., Lukina, M. M., Zagaynova, E. V. and Kuimova, M. K.** (2017). Live cell imaging of viscosity in 3D tumour cell models. *Multi-Parametric Live Cell Microsc. 3D Tissue Models* **1035**, 143-153. doi:10.1007/978-3-319-67358-5_10

**Shrestha, S., Serafino, M. J., Rico-Jimenez, J., Park, J., Chen, X., Zhaorigetu, S., Walton, B. L., Jo, J. A. and Applegate, B. E.** (2016). Multimodal optical coherence tomography and fluorescence lifetime imaging with interleaved excitation sources for simultaneous endogenous and exogenous fluorescence. *Biomed. Opt. Exp.* **7**, 3184-3197. doi:10.1364/BOE.7.003184

**Singh, M., Raghunathan, R., Piazza, V., Davis-Loiacono, A. M., Cable, A., Vedakkan, T. J., Janecek, T., Frazier, M. V., Nair, A., Wu, C. et al.** (2016). Applicability, usability, and limitations of murine embryonic imaging with optical coherence tomography and optical projection tomography. *Biomed. Opt. Exp.* **7**, 2295-2310. doi:10.1364/BOE.7.002295

**Sinsuebphon, N., Rudkouskaya, A., Barroso, M. and Intes, X.** (2018). Comparison of illumination geometry for lifetime-based measurements in whole-body preclinical imaging. *J. Biophotonics* **11**, e201800037. doi:10.1002/jbio.201800037

**Skala, M. C., Riching, K. M., Bird, D. K., Gendron-Fitzpatrick, A., Eickhoff, J., Eliceiri, K. W., Keely, P. J. and Ramanujam, N.** (2007). In vivo multiphoton fluorescence lifetime imaging of protein-bound and free nicotinamide adenine dinucleotide in normal and precancerous epithelia. *J. Biomed. Opt.* **12**, 024014. doi:10.1117/1.2717503

**Skruzny, M., Pohl, E., Gnoth, S., Malengo, G. and Sourjik, V.** (2020). The protein architecture of the endocytic coat analyzed by FRET microscopy. *Mol. Syst. Biol.* **16**, e9009. doi:10.15252/msb.20199009

**Smith, J. T., Yao, R., Sinsuebphon, N., Rudkouskaya, A., Un, N., Mazurkiewicz, J., Barroso, M., Yan, P. and Intes, X.** (2019). Fast fit-free analysis of fluorescence lifetime imaging via deep learning. *Proc. Natl. Acad. Sci. USA* **116**, 24019-24030. doi:10.1073/pnas.1912707116

**Smith, J. T., Aguénounon, E., Gioux, S. and Intes, X.** (2020a). Macroscopic fluorescence lifetime topography enhanced via spatial frequency domain imaging. *Opt. Lett.* **45**, 4232-4235. doi:10.1364/OL.397605
**Smith, J. T., Ochoa, M. and Intes, X.** (2020b). UNMIX-ME: spectral and lifetime fluorescence unmixing via deep learning. *Biomed. Opt. Exp.* **11**, 3857-3874. doi:10.1364/BOE.391992
**Soll, D. R. and Daniels, K. J.** (2016). Plasticity of Candida albicans biofilms. *Microbiol. Mol. Biol. Rev.* **80**, 565-595. doi:10.1128/MMBR.00068-15
**Sosnik, J., Zheng, L., Rackauckas, C. V., Digman, M., Gratton, E., Nie, Q. and Schilling, T. F.** (2016). Noise modulation in retinoic acid signaling sharpens segmental boundaries of gene expression in the embryonic zebrafish hindbrain. *eLife* **5**, e14034. doi:10.7554/eLife.14034
**Sparks, H., Kondo, H., Hooper, S., Munro, I., Kennedy, G., Dunsby, C., French, P. and Sahai, E.** (2018). Heterogeneity in tumor chromatin-doxorubicin binding revealed by in vivo fluorescence lifetime imaging confocal endomicroscopy. *Nat. Commun.* **9**, 2662. doi:10.1038/s41467-018-04820-6
**Stark, M., Manz, B., Ehlers, A., Küppers, M., Riemann, I., Volke, F., Siebert, U., Weschke, W. and König, K.** (2007). Multiparametric high-resolution imaging of barley embryos by multiphoton microscopy and magnetic resonance micro-imaging. *Microsc. Res. Tech.* **70**, 426-432. doi:10.1002/jemt.20426
**Staudinger, C. and Borisov, S. M.** (2015). Long-wavelength analyte-sensitive luminescent probes and optical (bio)sensors. *Methods Appl. Fluorescence* **3**, 042005. doi:10.1088/2050-6120/3/4/042005
**Steinegger, A., Wolfbeis, O. S. and Borisov, S. M.** (2020). Optical sensing and imaging of pH values: spectroscopies, materials, and applications. *Chem. Rev.* **120**, 12357-12489. doi:10.1021/acs.chemrev.0c00451
**Steinmark, I. E., James, A. L., Chung, P.-H., Morton, P. E., Parsons, M., Dreiss, C. A., Lorenz, C. D., Yahioglu, G., Suhling, K.** (2019). Targeted fluorescence lifetime probes reveal responsive organelle viscosity and membrane fluidity. *PLoS ONE* **14**, e0211165. doi:10.1371/journal.pone.0211165
**Steuwe, C., Vaeyens, M.-M., Jorge-Peñas, A., Cokelaere, C., Hofkens, J., Roeffaers, M. B. J. and van Oosterwyck, H.** (2020). Fast quantitative time lapse displacement imaging of endothelial cell invasion. *PLoS ONE* **15**, e0227286. doi:10.1371/journal.pone.0227286
**Stöckl, M. T., Bizzarri, R. and Subramaniam, V.** (2012). Studying membrane properties using fluorescence lifetime imaging microscopy (FLIM). *Fluoresc. Methods Study Biol. Membr.* **13**, 215-240. doi:10.1007/4243_2012_48
**Stringari, C., Cinquin, A., Cinquin, O., Digman, M. A., Donovan, P. J. and Gratton, E.** (2011). Phasor approach to fluorescence lifetime microscopy distinguishes different metabolic states of germ cells in a live tissue. *Proc. Natl Acad. Sci. USA* **108**, 13582-13587. doi:10.1073/pnas.1108161108
**Stringari, C., Edwards, R. A., Pate, K. T., Waterman, M. L., Donovan, P. J. and Gratton, E.** (2012). Metabolic trajectory of cellular differentiation in small intestine by Phasor Fluorescence Lifetime Microscopy of NADH. *Sci. Rep.* **2**, 568. doi:10.1038/srep00568
**Sud, D., Mehta, G., Mehta, K., Linderman, J., Takayama, S. and Mycek, M.-A.** (2006). Optical imaging in microfluidic bioreactors enables oxygen monitoring for continuous cell culture. *J. Biomed. Opt.* **11**, 050504. doi:10.1117/1.2355665
**Suhling, K., Hirvonen, L. M., Becker, W., Smietana, S., Netz, H., Milnes, J., Conneely, T., Le Marois, A., Jagutzki, O., Festy, F. et al.** (2019). Wide-field time-correlated single photon counting-based fluorescence lifetime imaging microscopy. *Nuclear Instruments Methods Physi. Res. Sec. A Accelerators Spectrometers Detectors Assoc. Equip.* **942**, 162365. doi:10.1016/j.nima.2019.162365
**Szulczewski, J. M., Inman, D. R., Entenberg, D., Ponik, S. M., Aguirre-Ghiso, J., Castracane, J., Condeelis, J., Eliceiri, K. W. and Keely, P. J.** (2016). In vivo visualization of stromal macrophages via label-free FLIM-based metabolite imaging. *Sci. Rep.* **6**, 25086. doi:10.1038/srep25086
**Teodori, L., Crupi, A., Costa, A., Diaspro, A., Melzer, S. and Tarnok, A.** (2017). Three-dimensional imaging technologies: a priority for the advancement of tissue engineering and a challenge for the imaging community. *J. Biophoton.* **10**, 24-45. doi:10.1002/jbio.201600049
**Thaa, B., Herrmann, A. and Veit, M.** (2010). Intrinsic cytoskeleton-dependent clustering of influenza virus M2 protein with hemagglutinin assessed by FLIM-FRET. *J. Virol.* **84**, 12445-12449. doi:10.1128/JVI.01322-10
**Thiele, J. C., Helmerich, D. A., Oleksiievets, N., Tsukanov, R., Butkevich, E., Sauer, M., Nevskyi, O. and Enderlein, J.** (2020). Confocal fluorescence-lifetime single-molecule localization microscopy. *ACS Nano* **14**, 14190-14200. doi:10.1021/acsnano.0c07322
**Tian, L., Hires, S. A. and Looger, L. L.** (2012). Imaging neuronal activity with genetically encoded calcium indicators. *Cold Spring Harb. Protoc.* **2012**, pdb.top069609. doi:10.1101/pdb.top069609
**Timpson, P., Mcghee, E. J. and Anderson, K. I.** (2011a). Imaging molecular dynamics in vivo–from cell biology to animal models. *J. Cell Sci.* **124**, 2877-2890. doi:10.1242/jcs.085191
**Timpson, P., Mcghee, E. J., Morton, J. P., von Kriegsheim, A., Schwarz, J. P., Karim, S. A., Doyle, B., Quinn, J. A., Carragher, N. O., Edward, M. et al.** (2011b). Spatial regulation of RhoA activity during pancreatic cancer cell invasion driven by mutant p53. *Cancer Res.* **71**, 747-757. doi:10.1158/0008-5472.CAN-10-2267
**Trampe, E., Koren, K., Akkineni, A. R., Senwitz, C., Krujatz, F., Lode, A., Gelinsky, M. and Kühl, M.** (2018). Functionalized Bioink with optical sensor nanoparticles for $O_2$ imaging in 3D-bioprinted constructs. *Adv. Funct. Mater.* **28**, 1804411. doi:10.1002/adfm.201804411
**Trinh, A. L., Ber, S., Howitt, A., Valls, P. O., Fries, M. W., Venkitaraman, A. R. and Esposito, A.** (2019). Fast single-cell biochemistry: theory, open source microscopy and applications. *Methods Appl. Fluoresc.* **7**, 044001. doi:10.1088/2050-6120/ab3bd2
**Vallmitjana, A., Torrado, B., Dvornikov, A., Ranjit, S. and Gratton, E.** (2020). Blind resolution of lifetime components in individual pixels of fluorescence lifetime images using the phasor approach. *J. Phys. Chem. B* **124**, 10126-10137. doi:10.1021/acs.jpcb.0c06946
**Vander Heiden, M. G., Cantley, L. C. and Thompson, C. B.** (2009). Understanding the Warburg effect: the metabolic requirements of cell proliferation. *Science* **324**, 1029-1033. doi:10.1126/science.1160809
**Venditti, R., Rega, L. R., Masone, M. C., Santoro, M., Polishchuk, E., Sarnataro, D., Paladino, S., D'Auria, S., Varriale, A., Olkkonen, V. M. et al.** (2019). Molecular determinants of ER-Golgi contacts identified through a new FRET-FLIM system. *J. Cell Biol.* **218**, 1055-1065. doi:10.1083/jcb.201812020
**Venugopal, V., Chen, J., Barroso, M. and Intes, X.** (2012). Quantitative tomographic imaging of intermolecular FRET in small animals. *Biomed. Opt. Exp.* **3**, 3161-3175. doi:10.1364/BOE.3.003161
**von Erlach, T. C., Bertazzo, S., Wozniak, M. A., Horejs, C.-M., Maynard, S. A., Attwood, S., Robinson, B. K., Autefage, H., Kallepitis, C., del Río Hernández, A. et al.** (2018). Cell-geometry-dependent changes in plasma membrane order direct stem cell signalling and fate. *Nat. Mater.* **17**, 237-242. doi:10.1038/s41563-017-0014-0
**Walczysko, P., Kuhlicke, U., Knappe, S., Cordes, C. and Neu, T. R.** (2008). In situ activity of suspended and immobilized microbial communities as measured by fluorescence lifetime imaging. *Appl. Environ. Microbiol.* **74**, 294-299. doi:10.1128/AEM.01806-07
**Walsh, A. J., Mueller, K. P., Tweed, K., Jones, I., Walsh, C. M., Piscopo, N. J., Niemi, N. M., Pagliarini, D. J., Saha, K. and Skala, M. C.** (2020). Classification of T-cell activation via autofluorescence lifetime imaging. *Nat. Biomed. Eng.* **5**, 77-88. doi:10.1038/s41551-020-0592-z
**Wang, X.-D. and Wolfbeis, O. S.** (2014). Optical methods for sensing and imaging oxygen: materials, spectroscopies and applications. *Chem. Soc. Rev.* **43**, 3666-3761. doi:10.1039/C4CS00039K
**Wang, X. F., Periasamy, A., Herman, B. and Coleman, D. M.** (1992). Fluorescence lifetime imaging microscopy (FLIM): instrumentation and applications. *Crit. Rev. Anal. Chem.* **23**, 369-395. doi:10.1080/10408349208051651
**Wang, H.-W., Ghukasyan, V., Chen, C.-T., Wei, Y.-H., Guo, H.-W., Yu, J.-S. and Kao, F.-J.** (2008). Differentiation of apoptosis from necrosis by dynamic changes of reduced nicotinamide adenine dinucleotide fluorescence lifetime in live cells. *J. Biomed. Opt.* **13**, 054011. doi:10.1117/1.2975831
**Wang, W., Douglas, D., Zhang, J., Kumari, S., Enuameh, M. S., Dai, Y., Wallace, C. T., Watkins, S. C., Shu, W. and Xing, J.** (2020). Live-cell imaging and analysis reveal cell phenotypic transition dynamics inherently missing in snapshot data. *Sci. Adv.* **6**, eaba9319. doi:10.1126/sciadv.aba9319
**Weber, P., Schickinger, S., Wagner, M., Angres, B., Bruns, T. and Schneckenburger, H.** (2015). Monitoring of apoptosis in 3D cell cultures by FRET and light sheet fluorescence microscopy. *Int. J. Mol. Sci.* **16**, 5375-5385. doi:10.3390/ijms16035375
**Weitsman, G., Mitchell, N. J., Evans, R., Cheung, A., Kalber, T. L., Bofinger, R., Fruhwirth, G. O., Keppler, M., Wright, Z. V. F., Barber, P. R. et al.** (2017). Detecting intratumoral heterogeneity of EGFR activity by liposome-based in vivo transfection of a fluorescent biosensor. *Oncogene* **36**, 3618-3628. doi:10.1038/onc.2016.522
**Wetzker, C. and Reinhardt, K.** (2019). Distinct metabolic profiles in Drosophila sperm and somatic tissues revealed by two-photon NAD(P)H and FAD autofluorescence lifetime imaging. *Sci. Rep.* **9**, 19534. doi:10.1038/s41598-019-56067-w
**Witte, R., Andriasyan, V., Georgi, F., Yakimovich, A. and Greber, U. F.** (2018). Concepts in light microscopy of viruses. *Viruses* **10**, 202. doi:10.3390/v10040202
**Wollman, A. J. M., Hedlund, E. G., Shashkova, S. and Leake, M. C.** (2020). Towards mapping the 3D genome through high speed single-molecule tracking of functional transcription factors in single living cells. *Methods* **170**, 82-89. doi:10.1016/j.ymeth.2019.06.021
**Won, Y., Park, B., Kim, I. and Lee, S.** (2016). Fluorescence lifetime measurement with confocal endomicroscopy for direct analysis of tissue biochemistry in vivo. *Heliyon* **2**, e00139. doi:10.1016/j.heliyon.2016.e00139
**Wu, P.-H., Gilkes, D. M. and Wirtz, D.** (2018). The biophysics of 3D cell migration. *Annu. Rev. Biophys.* **47**, 549-567. doi:10.1146/annurev-biophys-070816-033854
**Xue, R., Behera, P., Viapiano, M. S. and Lannutti, J. J.** (2013). Rapid response oxygen-sensing nanofibers. *Mater. Sci. Eng. C* **33**, 3450-3457. doi:10.1016/j.msec.2013.04.030
**Xue, R., Nelson, M. T., Teixeira, S. A., Viapiano, M. S. and Lannutti, J. J.** (2016). Cancer cell aggregate hypoxia visualized in vitro via biocompatible fiber sensors. *Biomaterials* **76**, 208-217. doi:10.1016/j.biomaterials.2015.10.055
**Yao, R., Ochoa, M., Yan, P. and Intes, X.** (2019). Net-FLICS: fast quantitative wide-field fluorescence lifetime imaging with compressed sensing-a deep learning approach. *Light Sci. Appl.* **8**, 26. doi:10.1038/s41377-019-0138-x

**Yazgan, G., Dmitriev, R. I., Tyagi, V., Jenkins, J., Rotaru, G.-M., Rottmar, M., Rossi, R. M., Toncelli, C., Papkovsky, D. B., Maniura-Weber, K.** and et al. (2017). Steering surface topographies of electrospun fibers: understanding the mechanisms. *Sci. Rep.* **7**, 158. doi:10.1038/s41598-017-00181-0

**Yellen, G. and Mongeon, R.** (2015). Quantitative two-photon imaging of fluorescent biosensors. *Curr. Opin. Chem. Biol.* **27**, 24-30. doi:10.1016/j.cbpa.2015.05.024

**Yoon, S., Kim, M., Jang, M., Choi, Y., Choi, W., Kang, S. and Choi, W.** (2020). Deep optical imaging within complex scattering media. *Nat. Rev. Phys.* **2**, 141-158. doi:10.1038/s42254-019-0143-2

**Yoshihara, T., Hirakawa, Y., Hosaka, M., Nangaku, M. and Tobita, S.** (2017). Oxygen imaging of living cells and tissues using luminescent molecular probes. *J. Photochem. Photobiol. C Photochem. Rev.* **30**, 71-95. doi:10.1016/j.jphotochemrev.2017.01.001

**Zhang, Y., Hato, T., Dagher, P. C., Nichols, E. L., Smith, C. J., Dunn, K. W. and Howard, S. S.** (2019). Automatic segmentation of intravital fluorescence microscopy images by K-means clustering of FLIM phasors. *Opt. Lett.* **44**, 3928-3931. doi:10.1364/OL.44.003928

**Zhao, M., Wan, X., Li, Y., Zhou, W. and Peng, L.** (2015). Multiplexed 3D FRET imaging in deep tissue of live embryos. *Sci. Rep.* **5**, 13991. doi:10.1038/srep13991

**Zherdeva, V. V., Kazachkina, N. I., Shcheslavskiy, V. I. and Savitsky, A. P.** (2018). Long-term fluorescence lifetime imaging of a genetically encoded sensor for caspase-3 activity in mouse tumor xenografts. *J. Biomed. Opt.* **23**, 035002. doi:10.1117/1.JBO.23.3.035002

**Zhou, X., Liang, H., Jiang, P., Zhang, K. Y., Liu, S., Yang, T., Zhao, Q., Yang, L., Lv, W., Yu, Q. et al.** (2016). Multifunctional phosphorescent conjugated polymer dots for hypoxia imaging and photodynamic therapy of cancer cells. *Adv. Sci.* **3**, 1500155. doi:10.1002/advs.201500155

**Zhou, J., del Rosal, B., Jaque, D., Uchiyama, S. and Jin, D.** (2020). Advances and challenges for fluorescence nanothermometry. *Nat. Methods* **17**, 967-980. doi:10.1038/s41592-020-0957-y

**Zirath, H., Rothbauer, M., Spitz, S., Bachmann, B., Jordan, C., Müller, B., Ehgartner, J., Priglinger, E., Mühleder, S., Redl, H. et al.** (2018). Every breath you take: non-invasive real-time oxygen biosensing in two- and three-dimensional microfluidic cell models. *Front. Physiol.* **9**, C1527. doi:10.3389/fphys.2018.00815